Use of Functional Data to Model the Trajectory of an Inertial Measurement Unit and Classify Levels of Motor Impairment for Stroke Patients

使用功能数据来模拟惯性导航系统的轨迹，并对中风患者的运动损伤水平进行分类

Yi-Ting Hwang, Wei-An Lu, and Bor-Shing Lin, *Senior Member, IEEE*
黄一廷、卢伟安及林宝成，IEEE 高级成员

***Abstract* — Motor impairment evaluations are key rehabilitation-related assessments for patients with stroke. Currently, such evaluations are subjective; they are based on physicians' judgements regarding the actions performed by patients. This leads to inconsistent clinical results. Many inertial sensing elements for motion detection have been designed. However, to more easily and rapidly evaluate motor impairment, we require a system that can collect data effectively to predict the degree of motor impairment. Lin *et al.* used data gloves equipped with an inertial measurement unit (IMU) to collect movement trajectories for motor impairment evaluations in patients with stroke. The present study used functional data analysis to model data trajectories to reduce the influence of noise from IMU data and proposed using coefficients of function as features for classifying motor impairment. To verify the appropriateness of feature construction, five classification methods were used to evaluate the extracted features in terms of the overall and sensor-specific ability to classify levels of motor impairment. The results indicated that the features derived from cubic smoothing splines could effectively reflect key data characteristics, and a support vector machine yielded relatively high overall and sensor-specific accuracy for distinguishing between levels of motion impairment in patients with stroke. Future data glove systems can contain cubic smoothing splines to extract hand function features and then classify motion impairment for appropriate rehabilitation programs to be prescribed.**

摘要*—运动障碍评估是中风患者重要的康复相关评估。目前，这种评估是主观的，它们基于医生对患者行为的判断。这导致临床结果不一致。已经设计了许多用于动作感应的惯性元件。然而，为了更容易更迅速地评估运动损伤，我们需要一个能够有效收集数据来预测运动损伤程度的系统。Lin 等人使用装有惯性导航系统(IMU)的数据手套来收集运动轨迹，用于评估中风患者的运动损伤。本研究采用功能数据分析方法对数据轨迹进行建模，以降低 IMU 数据噪声的影响，并提出以功能系数作为运动损伤的分类特征。为了验证特征结构的合理性，采用五种分类方法对提取的特征进行综合评价和传感器特异性运动损伤分类能力评价。结果表明，三次平滑样条函数提取的特征能够有效地反映关键数据的特征，支持向量机对脑卒中患者运动障碍程度的判别具有较高的整体准确性和传感器特异性。未来的数据手套系统可以包含三次平滑样条来提取手功能特征，然后将运动障碍分类为适当的康复计划进行规定。

***Index Terms*— Functional data, inertial measurement unit, motor impairment, spline, stroke.**
功能数据、惯性导航系统、运动损伤、样条、冲程。

Manuscript received September 16, 2021; revised January 6, 2022 and February 27, 2022; accepted March 21, 2022. Date of publication March 25, 2022; date of current version April 18, 2022. This work was supported in part by the Ministry of Science and Technology in Taiwan under Grant MOST 109-2314-B-305-001 and Grant MOST 109-2221-E-305-001-MY2, in part by the University System of the Taipei Joint Research Program under Grant USTP-NTPU-TMU-109-03, in part by the Faculty Group Research Funding Sponsorship by the National Taipei University under Grant 2021-NTPU-ORDA-02, and in part by the "Academic Top-Notch and Features Field Project" funding sponsorship from the National Taipei University under Grant 109-NTPU_ORDA-F-005. *(Corresponding author: Bor-Shing Lin.)*

手稿于 2021 年 9 月 16 日收到; 2022 年 1 月 6 日和 2022 年 2 月 27 日修订; 于 2022 年 3 月 21 日接受。出版日期 2022 年 3 月 25 日; 当前版本日期 2022 年 4 月 18 日。这项工作部分得到了台湾科学技术部的资助，获得了 mos109-2314-b-305-001 和 mos109-2221-e-305-001-my2 资助，部分得到了台北大学联合研究计划大学系统的资助，获得了国立台北大学 2021-ntpu-orda-02 资助下的教员小组研究资助，部分得到了国立台北大学 109-ntpu _ orda-f-005 资助下的"学术一流和特色领域项目"资助。(通讯作者: Bor-Shing Lin

This work involved human subjects or animals in its research. Approval of all ethical and experimental procedures and protocols was granted by the Ethics Committee of Chi-Mei Hospital under IRB No. 10102-019.

这项工作涉及到人或动物的研究。根据 IRB no. 10102-019，奇美医院伦理委员会批准了所有伦理和实验程序和方案。

Yi-Ting Hwang and Wei-An Lu are with the Department of Statis-tics, National Taipei University, New Taipei City 23741, Taiwan (e-mail: hwangyt@gm.ntpu.edu.tw; vivialex96@gmail.com).

国立台北大学统计学系，台湾新北市 23741(电邮: hwangyt@gm.ntpu.edu.tw; vivialex96@gmail. com)。

Bor-Shing Lin is with the Department of Computer Science and Information Engineering, National Taipei University, New Taipei City 23741, Taiwan (e-mail: bslin@mail.ntpu.edu.tw).

林博成，国立台北大学计算机科学与信息工程系，台湾新北市 23741，电邮: bslin@mail.ntpu.edu.tw。

Digital Object Identifier 10.1109/TNSRE.2022.3162416
数字对象标识符 10.1109/TNSRE. 2022.3162416 doi

I. Introduction
引言

CEREBROVASCULAR diseases (CVDs), the leading cause of death and disability worldwide, were responsi-ble for an estimated 17.9 million deaths globally in 2019 [1].
脑血管疾病是世界范围内导致死亡和残疾的主要原因，2019 年全球估计有 1790 万人死亡[1]。

According to data from the Taiwanese government and in 2020, CVDs were the fourth leading cause of death and approximately 50.1 of 100000 Taiwanese residents died of CVDs [2]. Nevertheless, the number of stroke survivors has been increasing owing to considerable improvements in acute medical care. As such, the need for rehabilitation to restore physical function has dramatically increased. Approx-imately two-thirds of survivors can walk independently after a stroke [3], [4], but less than half of them regain basic upper limb function within a year of rehabilitation [5]. Stroke limits their independence in activities of daily living and reduces their quality of life. Thus, upper limb rehabilitation is crucial for stroke survivors.
根据台湾政府和 2020 年的数据，心血管疾病是第四大死因，10 万台湾居民中约有 50.1 人死于心血管疾病[2]。尽管如此，由于急性医疗保健的显着改善，中风幸存者的数量一直在增加。因此，恢复身体功能的康复需求显着增加。大约三分之二的幸存者在中风后能够独立行走，但是只有不到一半的人在康复后的一年内恢复了基本的上肢功能。中风限制了他们在日常生活活动中的独立性，降低了他们的生活质量。因此，上肢康复对中风幸存者至关重要。

Appropriate rehabilitation can effectively aid patients in achieving favorable recovery that enables them to perform functional activities. A person's rehabilitation plan is related to their disability level. Clinical methods are available for evalu-ating functional recovery, including the Fugl-Meyer test, action research arm test, box and block test, Jebsen–Taylor hand function test, and Brunnstrom stage (BS) test. As demonstrated by [6], the outcomes of the Fugl-Meyer test, action research arm test, and box and block test are strongly correlated, and these tests have high test–retest reliability according to stan-dardized guidelines. However, these clinical evaluation meth-ods are subjective, and scores for the same patient can vary among clinicians. Furthermore, without detailed movement-related information, providing an individualized rehabilitation plan can be difficult [7].

适当的康复可以有效地帮助患者实现有利的恢复，使他们能够进行功能活动。一个人的康复计划与他们的残疾水平有关。临床上常用的功能恢复评估方法包括 Fugl-Meyer 试验、动作研究臂试验、 box 和 block 试验、 Jebsen-Taylor 手功能试验和 Brunnstrom 分期试验。正如文献[6]所示，Fugl-Meyer 测验、行动研究臂测验、盒测验和块测验的结果具有很强的相关性，并且这些测验依据标准化指南具有较高的重测信度。然而，这些临床评估方法是主观的，同一患者的评分可能因临床医生而异。此外，没有详细的运动相关信息，提供个性化的康复计划可能是困难的[7]。

To reduce the burden on clinicians and improve the quality of care, more accurate and efficient evaluations are required for quantifying disability levels. Several tools for evaluating upper limb and hand functions have been developed in recent years. [8] designed a triaxial accelerometer-based system to quantify the clinical features of Parkinson disease. [9], [10] have used magnetic and inertial sensors to collect data when patients performed the Movement Disorder Society–Unified Parkinson's Disease Rating Scale finger tapping (FT) task, and [11] used inertial sensors to collect data and determine the

为了减轻临床医生的负担和提高护理质量，需要进行更准确和有效的评估，以量化残疾程度。近年来已经开发了几种评估上肢和手功能的工具。[8]设计了一个基于三轴加速度计的系统来量化帕金森氏症的临床特征。[9]，[10]使用磁性和惯性传感器收集数据时，患者执行运动障碍协会-统一帕金森病评定量表(FT)的任务，[11]使用惯性传感器收集数据和确定

features of parkinsonian tremors. Additionally, [12] designed and implemented a smartphone-based system for automated motor assessment by using low-cost off-the-shelf inertial sensors for measuring the movement of the joint angle of the upper body in patients with stroke. Furthermore, [13] designed an inexpensive and portable motion capture system by using a single reflective marker on the wrist to measure the kinematic movements of stroke survivors. For measuring hand kinematics, [14]–[17] have designed data gloves with inertial and magnetic sensors to detect joint movements in various directions.

帕金森病震颤的特征。此外，[12]设计和实施了一个基于智能手机的自动运动评估系统，利用低成本现成的惯性传感器测量中风患者上身关节角度的运动。此外，[13]设计了一个便宜的便携式运动捕捉系统，通过使用手腕上的一个反射标记来测量中风幸存者的运动学运动。为了测量手部运动学，[14]-[17]设计了具有惯性和磁性传感器的数据手套，以检测各个方向的关节运动。

Sensors can be easily used to collect a large amount of data. Depending on the number of sensors and recording time, various functional trajectories are available for each participant. To conduct further analyses, these variable trajectories must be manipulated. [13] introduced five components, which were crudeness, two speed profile deviations, smoothness, and segmentation, to capture variable trajectories, and these components were measured using confidence scores, which required a reference trajectory and several threshold values. On the basis of physical characteristics, [16] developed only three features, namely average rotation speed, variations in movement completion time, and quality of movement, from raw data. [18] computed summary statistics, such as centrality and variablity, and the extremes of variable trajectories, which yielded over 3000 features. Related raw data were collected from signals transmitted from multiple devices, and data spikes, packet loss, and data gaps were noted when the server could not receive and process data instantly [19]. Furthermore, an inherent deficiency in related devices, such as clock stretch-ing, can result in sporadic incorrect data points [20]. These outliers greatly affect the accuracy of summary statistics, especially extreme values.

传感器可以很容易地用来收集大量的数据。根据传感器的数量和记录时间，各种功能轨迹可用于每个参与者。为了进一步分析，必须操纵这些可变轨迹。[13]引入了粗糙度、两个速度剖面偏差、平滑度和分割五个分量来捕捉可变轨迹，这些分量使用置信度分数来测量，这些分量需要一个参考轨迹和几个阈值。在物理特征的基础上，[16]从原始数据中只发展出三个特征，即平均旋转速度、运动完成时间的变化和运动质量。[18]计算总结统计，如中心性和可变性，以及可变轨迹的极端，产生了超过 3000 个特征。从多个设备传输的信号中收集相关的原始数据，当服务器无法立即接收和处理数据时，会注意到数据峰值、数据包丢失和数据间隙[19]。此外，相关设备(如时钟延长)的固有缺陷可能导致零星的不正确数据点[20]。这些异常值极大地影响了汇总统计的准确性，特别是极值。

Only some data trajectories have been examined in the literature. This study introduced a functional analysis that can capture entire data trajectories. Through a prespecified basis function and an objective function, a functional form is used to fit data trajectories. Instead of processing raw data, this functional form eliminates the noise induced by data collection [21]. This study investigated the feasibility of using functional analysis to analyze sensor data. Unlike summary statistics, which require the use of principle component analysis (PCA) to reduce the number of features [18], in functional analysis, the number of features depends on the number of bases and is determined objectively through crossvalida-tion. The feasibility of features derived from the functional approach was demonstrated by evaluating the accuracy in determining patients' motor impairment level using the data collected by [16]. Furthermore, because these features provide sufficient information on data trajectories, the importance of sensors was also examined, and the results can further reduce the cost of developing data gloves.

文献中只检查了一些数据轨迹。这项研究引入了一个功能分析，可以捕获整个数据轨迹。通过预先指定的基函数和目标函数，使用函数形式来拟合数据轨迹。这种功能形式不是处理原始数据，而是消除了数据收集引起的噪声[21]。这项研究调查了使用功能分析来分析传感器数据的可行性。概要统计需要使用主成分分析(PCA)来减少特征的数量[18]，而在功能分析中，特征的数量取决于碱基的数量，通过交叉验证客观地确定。通过使用[16]收集的数据评估确定患者运动损伤程度的准确性，证明了功能方法特征的可行性。此外，由于这些特征提供了关于数据轨迹的充分信息，因此还研究了传感器的重要性，结果可以进一步降低开发数据手套的成本。

II. Methods
方法

A. Participants
A. 参与者

This study enrolled 15 patients with stroke and 15 healthy age-matched individuals (H). The inclusion criteria for the study were 1) age of 20–80 years and 2) the ability to maintain

本研究纳入了 15 例脑卒中患者和 15 例年龄匹配的健康个体(h)。该研究的纳入标准是 1)20-80 岁的年龄和 2)维持能力

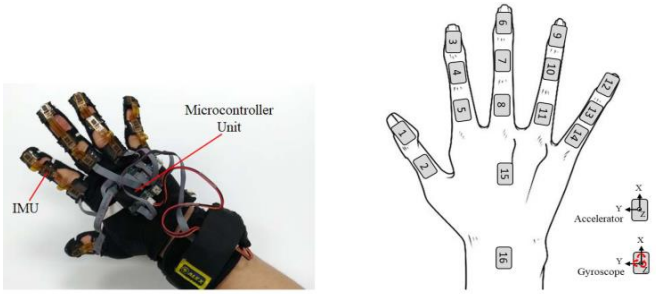

(a) Data glove (b) Positions

Fig. 1. (a) Photograph of the data glove. (b) Positions of the IMU sensors.
图 1。(a)数据手套的照片。(b) IMU 传感器的位置。

a sit-up position for longer than 40 min. The exclusion criteria included 1) a diagnosis of hemispatial akinesia or visual attention deficit, 2) cognitive impairment, 3) joint defects in the upper extremities prior to a stroke. In this study, the BS test was used to evaluate motor impairment level. Of the 15 patients with stroke, 4 had BS4, 10 had BS5, and 1 had BS6. A therapist determined and provided patients' BS as the ground truth for classification. Because patients at BS6 with stroke typically have hand function that is clinically similar to that of healthy individuals, the patient with BS6 was treated as a healthy individual.

仰卧起坐超过 40 分钟。排除标准包括: 1)诊断为偏侧运动障碍或视觉注意缺陷，2)认知障碍，3)中风前上肢关节缺损。在这项研究中，BS 测试被用来评估运动障碍水平。在 15 例卒中患者中，4 例有 BS4,10 例有 BS5,1 例有 BS6。治疗师确定并提供患者的 BS 作为分类的基本事实。由于 bs6 型脑卒中患者的手功能在临床上与健康人相似，因此 bs6 型脑卒中患者被视为健康人。

The average ages for healthy individuals and patients were 62.6 and 59.3 years, respectively. Nine patients and five healthy participants were men. This study was performed at Chi-Mei Hospital, Tainan, Taiwan, and was approved by the Ethics Committee of Chi-Mei Hospital (IRB No. 10102-019). All participants provided written informed consent.

健康个体和患者的平均年龄分别为 62.6 岁和 59.3 岁。9 名患者和 5 名健康参与者是男性。本研究在台湾台南市 Chi-Mei 医院进行，并获得 Chi-Mei 医院伦理委员会(IRB no. 10102-019)的批准。所有参与者均提供书面知情同意书。

B. Device and Task
B. 设备和任务

Self-developed data gloves containing 16 inertial measurement units (IMUs; LSM330DLC; STMicroelectronics, Geneva, Switzerland) were used for data collection. A gyroscope and an accelerometer were included in each IMU to capture data on triaxial angular velocity and acceleration. The IMU data were collected by a microcontroller unit (MSP430; Texas Instruments, Dallas, TX, USA) and were wirelessly transmitted as encapsulated packets to a laptop through a Bluetooth interface. Fig. 1 (a) presents a photograph of the data glove, and Fig. 1 (b) displays the IMU sensor positions on the glove. The detailed mechanical design is provided in [16].

自行研制的数据手套包含 16 个惯性测量单元(IMUs; LSM330DLC; stmicroelectronics，瑞士日内瓦)用于数据采集。在每个 IMU 中包括陀螺仪和加速度计以捕获三轴角速度和加速度的数据。IMU 数据由微控制器单元(MSP430; Texas Instruments，Dallas，TX，USA)收集，并通过蓝牙接口以封装包的形式无线传输到笔记本电脑。图 1(a)显示了数据手套的照片，图 1(b)显示了手套上的 IMU 传感器位置。详细的机械设计在[16]中提供。

All participants were asked to wear the data glove to detect their hand motions when performing a thumb task (TT) and a grip task (GT). The tools for these tasks are illustrated in Fig. 2. The TT was designed to evaluate thumb dexterity. In this task, each participant was asked to hold a cylinder in their hand [Fig. 2 (a)] and then use their thumb to repeatedly push a button on the cylinder. A complete motion was defined as the completion of a press and release action. The GT was aimed at assessing the dexterity of the entire hand. For this task, each participant was asked to perform a grip and release motion using the tool displayed in Fig. 2 (b). The grip and release motions constituted a single complete motion. For both the GT and TT, each participant was asked to perform a complete motion within 4 s and repeat it ten times. For the TT and GT, a complete motion comprised ten cycles.

所有参与者都被要求戴上数据手套，以检测他们在执行拇指任务(TT)和握力任务(GT)时的手部动作。这些任务的工具如图 2 所示。TT 旨在评估拇指的灵活性。在这个任务中，每个参与者被要求手持一个圆柱体[图 2(a)]，然后用他们的拇指重复按下圆柱体上的一个按钮。一个完整的动作被定义为完成一个新闻和释放动作。GT 旨在评估整个手的灵活性。对于这项任务，要求每个参与者使用图 2(b)中显示的工具执行握力和释放动作。握力和释放动作构成了单个完整的动作。对于 GT 和 TT，每个参与者被要求在 4 秒内完成一个完整的动作，并重复 10 次。对于 TT 和 GT，一个完整的动作由十个周期组成。

(a) (b)

Fig. 2. (a) TT and (b) GT tools.
图 2。(a) TT 和(b) GT 工具。

TABLE I
表 i
DATA RECORDING
数据记录

Thumb task (TT)	29	23	8	60
Grip task (GT)	33	22	8	63
Total	62	45	16	123

Depending on their physical condition, each participant was asked to repeat each task two or three times. In total, 60 and 63 sets of measurements were obtained for the TT and GT, respectively, and 62 and 61 sets of measurements were obtained from healthy individuals and patients with stroke, respectively (Table I). The data were collected from 16 IMU sensors. Furthermore, acceleration and angular velocity in three dimensions were extracted for each sensor.

根据他们的身体状况，每个参与者被要求重复每个任务两到三次。总共获得了 60 组 TT 和 63 组 GT 测量数据，62 组和 61 组测量数据分别来自健康个体和脑卒中患者(表 i)。数据来自 16 个 IMU 传感器。此外，为每个传感器提取三维加速度和角速度。

C. Data Analysis
C. 数据分析

Because the sensors collected data every 23 ms, the data were manually divided into ten cycles to exclude the influence of between-cycle data. Although the participants were instructed to complete both the TT and GT in 4-s cycles, the actual cycle duration varied among them. To determine the acceleration and angular velocity trajectories, the time space was adjusted to [0, 1]. These trajectories were thus a function of time, and functional data analysis could be used to model the data trajectories.

$l = 1, \ldots, T$ (called knots) and t_0 denotes the lower bound of the time interval. For a subinterval (t_l, t_{l+1}), a truncated power function of order d is used as follows:
= 1，...，t (称为节点)和 t0 表示时间间隔的下界。对于子区间(tl，tl + 1)，使用 d 阶截断的幂函数如下:

$$\varphi_j(t) = t_j - 1,\ 1 \le j \le (d+1) \quad (3)$$
$$\Phi_j(t) = t_j\text{-}1,\ 1 \le j \le (d+1) \quad (3)$$
$$\varphi_{d+j}(t) = (t - t_j)+d,\ 1 \le j \le T, \quad (4)$$
$$\Phi_{d+j}(t) = (t\text{-}t_j) + d,\ \ 1 \le j \le t, \quad (4)$$

where $(t)+ = t$ if $t > 0$; otherwise, $(t)+ = 0$. The number of parameters is $(d + 1) \times (T + 1) - T \times d = d + T + 1$. According to [22], a cubic spline ($d = 3$) is sufficient to fit the data trajectory properly when a sufficient number of knots is considered. The bases are presented as follows: $\varphi_1(t) = 1$,
其中(t) + = t，如果 t > 0; 否则，(t) + = 0。参数的数量是(d + 1) ×(t + 1)-t ×d = d + t + 1。根据[22]，当考虑足够数量的节点时，三次样条函数(d = 3)足以适当地拟合数据轨迹。基数表示如下: φ1(t) = 1,

$\varphi_2(t) = t$,
$\Phi_2(t) = t$,

$$\varphi_{j+2}(t) = d_j(t) - dT_{-1}(t),\ 1 \le j \le T-2, \quad (5)$$
$$\varphi_{j+2}(t) = d_j(t)\text{-}dT\text{-}1(t),\ \ 1 \le j \le t\text{-}2, \quad (5)$$

where
在哪儿

$$d_j(t) = \frac{(t - t_j)_+^3 - (t - t_T)_+^3}{t_T - t_j} - \frac{(t_j\text{-}t)_+^3 - (t_T\text{-}t)_+^3}{t_T - t_j}. \quad (6)$$

是的 T j

Each of these basis functions satisfies $d_j(\cdot) = d_T(\cdot) = 0$.
每个基函数满足 d ( ) = d ( ) = 0。

To prevent the selection of a maximal set of knots, the penalized residual sum of squares was used as follows:
为了防止选择一组最大的节点，则惩罚剩余平方和的用法如下:

$$RSS(f, \lambda) = \sum_{i=1}^{N} (y_i - f(x_i))^2 + \lambda \int (f''(t))^2\,dt, \quad (7)$$
$$RSS(f, \lambda) = \sum_{I=1} (y_i\text{-}f(x_i))^2 + \lambda \int (f''(t))^2\,dt, \quad (7)$$

因为传感器每 23 毫秒收集一次数据，所以数据被手动划分为 10 个周期，以排除周期间数据的影响。尽管参与者被指示在 4-s 周期内完成 TT 和 GT，但实际的周期时间各不相同。为了确定加速度和角速度轨迹，将时间空间调整为[0,1]。因此，这些轨迹是时间的函数，功能性数据分析可以用来模拟数据轨迹。

Let y_i denote the outcome measured at time x_i, where $i = 1, \cdots, N$. The general model is expressed as follows:
让 yi 表示在时间 xi 测量的结果，其中 i = 1，...，n。一般模型表示如下:

where $\lambda \in (0, \infty)$, denoting a fixed smoothing parameter, is used to identify the estimator of c_j s. An explicit unique minimizer, a natural spline with knots at the unique values of i for i = 1, 2, . . . , N can be obtained as follows:
其中表示固定平滑参数的 λ ∈(0，∞)用于识别 c j s 的估计量。一个显式的唯一极小值，一个自然样条与节点的唯一值 i 为 i = 1,2，... ，n，可以得到如下：

$$f(t) = \sum_{j=1}^{N} \varphi_j(t) c_j, \quad (8)$$

$$F(t) = \sum_{j=1}^{N} \Phi_j(t) c_j, \quad (8)$$

$$y_i = f(x_i) + \varepsilon_i, \quad i = 1, \ldots, N, \quad (1)$$

$$是的 F(xi) 我 1, · · N, (1)$$

$$= + = ·$$

where f (·) is a prespecified smoothing function, N is the number of sample points, and ε_i denotes independent zero-mean random variables. The smoothing function is often expressed in terms of basis functions as follows:
其中 f (·)是预先指定的平滑函数，n 是 number 样本点的误差，以及 ε_i 表示独立的零均值 random variables. The smoothing function is often expressed 平滑函数经常用表达式表示 in terms of basis functions as follows: 基本职能如下：

$$f(t) = \sum_{j=1}^{k} \varphi_j(t) c_j, \quad (2)$$

$$F(t) = \sum_{j=1}^{k} \Phi_j(t) c_j, \quad (2)$$

where k is a prespecified number of bases, φ j (·) is a prespecified j th basis, and c_j is the corresponding j th coefficient.
其中 k 是预先设定的碱基数，φ j (·)是预先设定的碱基数 ified j th basis, and c j is the corresponding j th coefficient. J 基，c j 是相应的 j 系数。

Although the task motions were performed periodically, the duration of each cycle varied among participants. In this study, two basis systems were thus considered: truncated power base splines (i.e., regression splines; commonly used for nonperiodic functional data) and Fourier bases
尽管任务动作是定期执行的，但 持续时间 循环 不同的 参与者 这个 研究，因此考虑了两个基础系统: 截断 幂基样条函数(即回归样条函数;

where $\varphi_j(t)$ is an N-dimensional set of basis functions for natural splines. The criterion defined in (7) can be reduced as follows:
其中 φ j (t)是自然样条的 n 维基函数集。定义在(7)中的准则可以简化如下:

$$RSS(c, \lambda) = (y - c)(y - c) + \lambda c \varphi c, \quad (9)$$

$$RSS(c, \lambda) = (y-c)(y-c) + \lambda c \varphi c, \quad (9)$$

where $\{N_j(x_i)\} = \{N_j(x_i)\}$ and $\varphi_{jk} = \int \Phi_j(t) \varphi_k(t) dt$. The tuning parameter λ determines the smoothness of the fitted curve.
在哪儿 及 调谐参数 λ 决定了拟合的平滑度 曲线。

The multivariate adaptive regression spline procedure is then used to determine a suitable set of optimally positioned knots.
然后是多变量自适应回归样条程序 用于确定一组合适的最佳位置结。

The optimal value of λ is determined through generalized crossvalidation and is represented as
Λ 的最佳值是通过广义 交叉验证，表示为

$$GCV(\lambda) = \frac{\sum_{i=1}^{N} (y_i - \hat{f}_\lambda(x_i))^2}{(1 - M(\lambda)/N)^2}, \quad (10)$$

$$GCV(\lambda) = \frac{\sum_{i=1}^{N} (y_i - \hat{f}_\lambda(x_i))^2}{(1 - M(\lambda)/n)^2}, \quad (10)$$

where M(λ) is the effective number of parameters in the model including λ, number of knots, and the positions of the knots.
在哪儿 M (λ) 就是 有效 号码 参数 在 optimal 模特，包括 λ, 的 号码 打结，以及 the 最佳 状态 绳结的位置。

2) Fourier Series: A Fourier series uses sin and cos functions as the basis functions. In other words, we have φ2r−1(t) = sin(r ωt) and φ2r (t) = cos(r ωt), where ω represents
2)傅里叶级数: 傅里叶级数使用正弦函数和余弦函数 作为基函数，换句话说，我们有 φ2r-1(t) =

(commonly
用于非周期函数数据)和傅里叶基(通常
used for periodic functional
data).
用于周期性函数数据)。

1) Regression Splines: To define a polynomial spline, the
1)回归样条: 为了定义一个多项式样条,
range is first divided into
T
范围首先分为 t
disjoint subintervals by tl ,
where
通过 tl 不相交子区间，其中
the
Sin (r ωt)和 φ2r (t) = cos (r ωt)， 其中 ω 表示
period. The Fourier series is then defined as
follows:
周期。傅里叶级数定义如下:

$$f(t) = c0 + c1 \sin \omega t + c2 \cos \omega t + c3 \sin 2\omega t$$

$$f(t) = c0 + c1 \sin \omega t + c2 \cos \omega t + c3 \sin 2\omega t$$

$$+ c4 \cos 2\omega t + \cdots \quad (11)$$

$$+ c4 \cos 2\omega t + \ldots \quad (11)$$

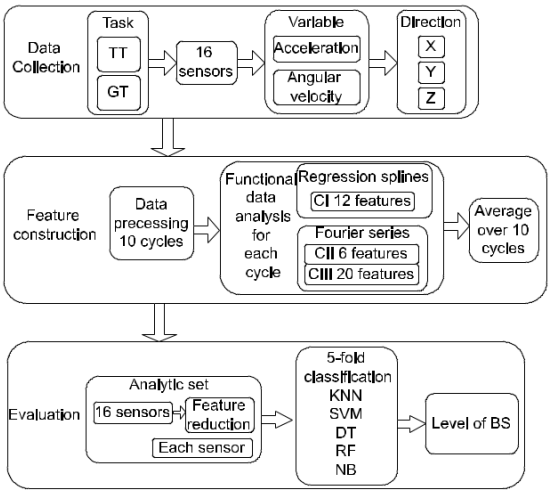

Fig. 3. Data analysis flowchart.
图 3。数据分析流程图。

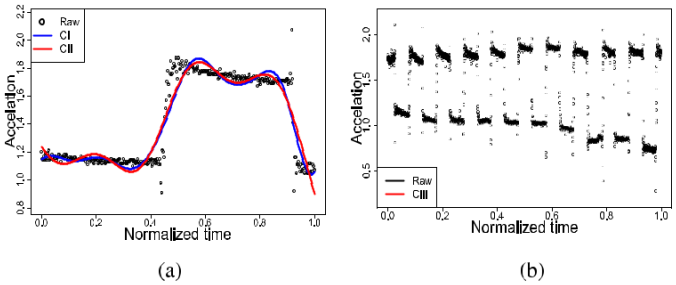

Fig. 4. Plot showing raw data, (a) the fitted smoothing spline and Fourier series for one cycle, and (b) Fourier series for ten cycles.
图 4。显示原始数据的图，(a)拟合的平滑样条和傅里叶一个周期的傅里叶级数和(b)十个周期的傅里叶级数。

TABLE II
表二
NUMBER OF ESSENTIAL FEATURES DERIVED FOR DIFFERENT MEASURES AND THE DIRECTIONS OF EACH CONSTRUCTION FROM THE TT AND GT
根据不同的衡量标准和每个标准的方向从 TT 和 GT 施工

D. Methodological Summary
D. 方法概要

As stated, in the GT and TT, a complete motion comprised ten cycles. A smoothing trajectory based on the regression spline was obtained for each of these cycles. For the Fourier series, a smoothing trajectory was obtained for each of these cycles and also for ten cycles. The feasibility of these fea-ture constructions for classifying the level of stroke-related motor impairment was evaluated using the *k*-nearest neighbor (KNN), support vector machine (SVM), decision tree (DT), random forest (RF), and naive Bayes classifier (NB) methods. The results of two assessments were considered. The first was an overall evaluation of the entire system, and the second was used examine the importance of each of the 16 sensors. Owing to the limited numer of measurements taken, feature reductions were required for the first assessment. Fig. 3 illustrates the flow of the data analysis.

如前所述，在 GT 和 TT 中，一个完整的动作由十个周期组成。基于回归样条的平滑轨迹得到了这些周期中的每一个。对于傅里叶级数，获得了这些周期中的每一个以及 10 个周期的平滑轨迹。采用 k- 最近邻(KNN)、支持向量机(SVM)、决策树(DT)、随机森林(RF)和朴素贝叶斯分类器(NB)方法，评价了这些特征结构对脑卒中相关运动损伤程度进行分类的可行性。考虑了两个评估的结果。第一个是对整个系统的整体评估，第二个是用来检查 16 个传感器中每个传感器的重要性。由于所采取的测量数量有限，第一次评估需要减少特征。图 3 说明了数据分析的流程。

1) Feature Construction: The regression spline was applied using the *smoothing.spline* package in R, and the default hyperparameters were used, except for the maximum number of knots (nknots). In this study, 10 knots was the maximum. The resulting smoothing splines had 12 coefficient estimates. For an individual variable, ten sets of coefficient estimates and their corresponding averages were obtained. This was the first feature type and was termed CI.

特征构造：使用 r 中的 smoothing.spline 软件包进行回归样条，并使用默认的超参数，但不包括最大节点数(nknot)。在这项研究中，10 节是最大的。由此产生的光滑样条有 12 个系数估计。对于一个单独的变量，获得了十组系数估计值及其相应的平均值。这是第一个特征类型，被称为 CI。

The Fourier function in R was used for data fitting. When the smoothing trajectory was being derived for only one cycle, three Fourier bases provided a satisfactory fit for each cycle and resulted in six coefficient estimates. The average estimates of six coefficients corresponding to ten cycles were then obtained. This was the second feature type and was termed CII.

R 中的傅里叶函数用于数据拟合。当平滑轨迹仅推导一个周期时，三个傅立叶基对每个周期提供了令人满意的拟合，并导致六个系数估计。然后获得对应于十个循环的六个系数的平均估计值。这是第二种特征类型，被称为 CII。

In accordance with the preliminary data exploration related to various bases, ten Fourier bases were selected for ten cycles and resulted in 20 coefficient estimates. This was the third feature type and was termed CIII. The fitted curves for acceleration are provided in Fig. 4 (a) and (b). These fitted curves could capture trajectories and were not influenced by outliers.

根据不同基数的初步数据探索，选取 10 个傅里叶基数进行 10 个周期，得到 20 个系数估计值。这是第三种特征类型，被称为 CIII。图 4(a)和(b)提供了加速度的拟合曲线。这些拟合曲线可以捕捉轨迹，不受异常值的影响。

2) Feature Reductions: In each recording, each of the 16 sensors collected data on six variables. In other words, data

特征减少：在每个记录中，16 个传感器中的每一个都收集了六个变量的数据。换句话说，数据

on 96 variables were collected in each recording. Feature construction was performed for each variable. The total number of CI, CII, and CIII features in each recording was equal to 96 variables multiplied by the number of coefficients for each construction, (1152, 576, and 1920, respectively). As indicated in Table I, the number of recordings was relatively small. To avoid overfitting in the classification, one-way analysis of variance and a Wilcoxon signed-rank test were performed to identify the essential features. Heat maps were generated to present the importance of features on the basis of these two tests. The columns present the features, and the rows present the triaxial (X, Y, and Z) acceleration (A) and angular velocity (G); all these data were captured by the 16 sensors. Different colors represent different levels of significance. A feature was regarded as essential if and only if both p values derived from these two tests were significant (< 0.05).

在每个记录中收集 96 个变量。对每个变量进行特征构建。每个记录中的 CI、 CII 和 CIII 特征的总数等于 96 个变量乘以每个结构的系数数目(分别为 1152、576 和 1920)。如表 i 所示，记录的数量相对较少。为了避免分类中的过拟合，采用单因素方差分析和威尔克科逊检验来识别本质特征。生成热图以在这两个测试的基础上显示特征的重要性。列表示特征，行表示三轴(x，y，z)加速度(a)和角速度(g)；所有这些数据都被 16 个传感器捕获。不同的颜色代表不同的重要性水平。一个特征被认为是必不可少的，当且仅当从这两个测试得出的两个 p 值都是显着的(< 0.05)。

Table II summarizes the number of essential features derived using different measures and the directions of CI, CII, and CIII from the TT and GT. For the TT, 25.5%, 20.7%, and 17.1% of the features constructed from CI, CII, and CIII, respectively, were identified as essential features. CI yielded a slightly larger number of essential features than did CII and CIII. Among the essential features in CI, 20.3% were derived from acceleration and were equally distributed in terms of direction. Two-thirds of the essential features derived from CII were also derived from acceleration but were primarily distributed in the X and Z directions. The essential features derived from CIII were obtained in equal number from acceleration and angular velocity. Most essential features obtained from acceleration were derived from the X and Z directions, whereas the largest number of essential

表 II 总结了使用不同测量方法得出的基本特征的数量以及 TT 和 GT 的 CI，CII 和 ciiii 的方向。在 TT 中，由 CI、 CII 和 ciiii 构建的特征分别有 25.5% 、20.7% 和 17.1% 被鉴定为基本特征。CI 产生的基本特征数量略多于 CII 和 CIII。在 CI 的基本特征中，20.3% 来源于加速度，并且在方向上均匀分布。来自 CII 的三分之二的基本特征也来源于加速度，但主要分布在 x 和 z 方向。从加速度和角速度获得等量的来自 ciiii 的基本特征。从加速度获得的大多数基本特征来自 x 和 z 方向，而最大数量的基本特征

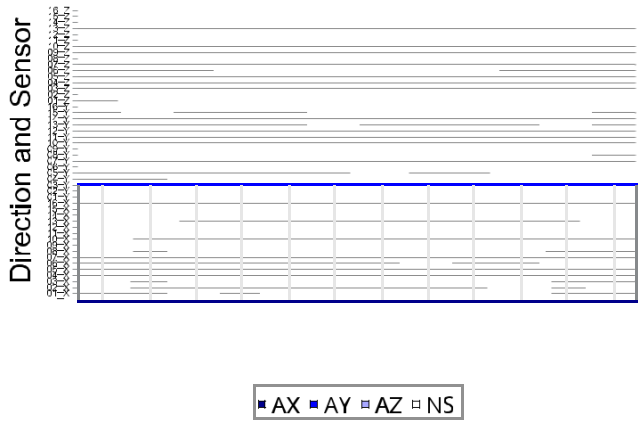

Fig. 5. Heat map of the *p* values of features constructed from CI on the basis of TT data, where colored areas represent essential features from different sensors and directions for A. NS denotes nonsignificance.
图 5。根据 TT 数据从 CI 构建的特征 p 值的热图，其中有色区域代表不同传感器和方向的基本特征。 NS 表示无意义。

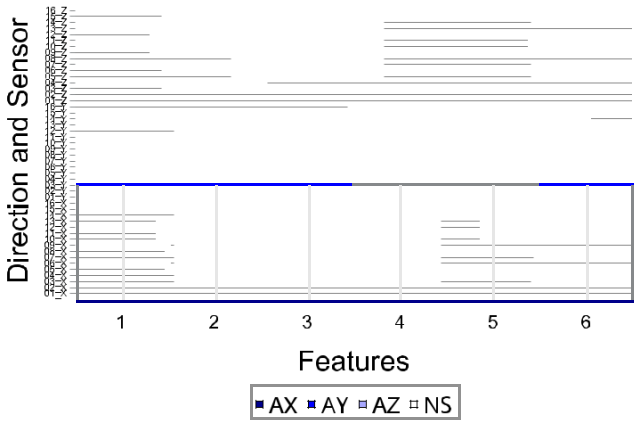

Fig. 6. Heat map of *p* values of features constructed from CII on the basis of TT data, where colored areas represent essential features from different sensors and directions for A. NS denotes nonsignificance.
图 6。根据 TT 数据从 CII 构建的特征 p 值的热图，其中有色区域代表不同传感器和方向的基本特征。 NS 表示无意义。

features obtained from angular velocity were derived from the
从角速度获得的特征来源于
Y direction.
方向。

For the GT, a larger number of essential features was provided; 41%, 42.4%, and 27.6% of such features were constructed from CI, CII and CIII, respectively. Different from the TT, for the GT, the number of essential features derived from acceleration and angular velocity were similar for all constructions. However, differences existed in their extraction in terms of direction. The essential features derived from acceleration were primarily collected from the *X* and *Z* directions, whereas those from G were from the *Y* direction. No essential feature was derived from the *X* direction for CIII.

对于 GT，提供了更多的基本特征，其中 41% 、42.4% 和 27.6% 的特征分别来自 CI、 CII 和 CIII。与 TT 不同的是，对于 GT，由加速度和角速度得到的基本特征的数量对于所有结构都是相似的。然而，它们在方向上的提取存在差异。来自加速度的基本特征主要从 x 和 z 方向收集，而来自 g 的基本特征来自 y 方向。Ciiii 的 x 方向没有衍生出基本特征。

The heat maps of the features related to the TT and GT are presented in Fig. 5; the columns contain information on the features and the rows contain information on measurements, directions, and sensors. Different colors are used to differentiate between the information presented in rows. Blue and red indicate essential features for A and G, respectively, and a gradient of colors from dark to light shades distinguishes between the *X* , *Y* , and *Z* directions.

与 TT 和 GT 相关的特征的热图如图 5 所示; 列包含特征的信息，行包含测量、方向和传感器的信息。不同的颜色被用来区分行中呈现的信息。蓝色和红色分别表示 a 和 g 的基本特征，从深色到浅色的颜色梯度区分 x、 y 和 z 方向。

The blue column in Fig. 5 represents approximately 80% of the essential features selected from A. The distribution of color depth was relatively uniform, and the colored column areas were more concentrated for sensors 3, 4, 5, 7, 10, and
图 5 中的蓝色列表示从 a 中选择的约 80% 的基本特征。颜色深度分布比较均匀，3、4、5、7、10 和 10 号传感器的色柱面积较集中
13. The blue columns have had an feature distribution, but the red columns had a higher concentration of features 5 and 10 (data not shown).
蓝色列具有特征分布，但红色列的特征 5 和 10 更集中(数据未显示)。

Most of the essential features for CII were features 1, 4, and 5 derived from the *X* and *Z* directions of A, as indicated in Fig. 6. For G, almost all six features were obtained from the *Y* direction of sensors 1, 2 and 3, and features 1–5 were obtained from the *Z* direction of sensors 3 and 4 (data not shown). For CIII, most of the essential features derived from A were features 11–20, and those from G were features 1–10 (data not shown).

CII 的大部分基本特征是特征 1、4 和 5，它们来源于 a 的 x 和 z 方向，如图 6 所示。对于 g，几乎所有的六个特征都是从传感器 1,2 和 3 的 y 方向获得的，而特征 1-5 是从传感器 3 和 4 的 z 方向获得的(数据未显示)。对于 CIII 来说，大部分来自 a 的基本特征是 11-20 的特征，而来自 g 的特征是 1-10 的特征(数据未显示)。

Fig. 7 (a) and (b) display the essential features for *A* and *G*, respectively. For A, all 12 features were essential features. They were derived from sensor 15 from the *X* direction; sensors 1, 2, 5, and 8 from the *Y* direction; and sensor 16 from the *Z* direction. In addition, 15 features from sensors 4, 7, 8,
图 7(a)和(b)分别显示了 a 和 g 的基本特征。对于 a 来说，所有 12 个特征都是基本特征。它们来自 x 方向的传感器 15，y 方向的传感器 1、2、5 和 8，以及 z 方向的传感器 16。此外，传感器 4、7、8 的 15 个特征，

10, 12, and 13 from the *Z* direction were essential features, and Feature 11 from sensors 1 and 3–15 from the *X* direction was an essential feature. As indicated in Table II, most of the essential features for G were derived from the *Y* direction [see Fig. 7 (b)]. Feature 6 from the *Y* direction of all sensors was determined to be essential. Except for feature 12, most of the other features from sensors 1–14 were determined to be essential.

z 方向的 10、12 和 13 是基本特征，x 方向的传感器 1 和 3-15 的特征 11 是基本特征。如表 II 所示，g 的大部分基本特征来源于 y 方向[参见图 7(b)]。所有传感器的 y 方向的特征 6 被确定为必不可少的。除了特征 12 之外，来自传感器 1-14 的大多数其他特征被认为是必不可少的。

For CII, all features from the *X* direction of sensors 4, 5, 8, 10, 11, 13, and 14 and the *Z* direction of sensors 3, 4, 6, 7, 9, 10, and 12 for A were essential features, as shown in Fig. 8. For G, all features from the *Y* direction of sensors 2, 5, and 8–14 were essential features, and all features from the *Z* direction of sensor 9 were essential features. A similar pattern was also observed for CIII (data not shown).

对于 CII，来自传感器 4、5、8、10、11、13 和 14 的 x 方向和传感器 3、4、6、7、9、10 和 12 对于 a 的 z 方向的所有特征都是基本特征，如图 8 所示。对 g 来说，传感器 2、5 和 8-14 的 y 方向的所有特征都是基本特征，而传感器 9 的 z 方向的所有特征都是基本特征。CIII 也观察到类似的模式(数据未显示)。

3) Evaluations: Classification procedures were performed separately for the TT and GT. The results from each classification are summarized in a confusion matrix. Let $n_{i\,j}$ represent the number of observations for the *i* th observed value and the *j* th predicted value, where 1, 2, and 3 represent individ-uals with a healthy status, BS5, and BS4, respectively [23]. The overall accuracy was determined by dividing the num- tions in identifying individuals without stroke, patients with BS5, and patients with BS4 was also computed. The accuracy in identifying individuals without stroke was determined by the number of correct predictions of individuals without stroke divided by the number of observations for that group. The other definitions were similar to the aforementioned one. Finally, the average overall accuracy was determined, as was the accuracy over 30 task repetitions by individuals without stroke, patients with BS5, and patients with BS4.

评估: 进行分类程序

分别为 TT 和 GT。每个分类的结果总结在一个混淆矩阵中。让 ni j 表示第 1 个观测值和第 1 个预测值的观测次数，其中 1、2 和 3 分别表示健康状态的个体，bs5 和 BS4[23]。总体准确性是通过除以识别没有卒中的个体，bs5 患者和 bs4 患者的数量来确定的。识别无卒中个体的准确性由无卒中个体的正确预测数量除以该组的观察数量来确定。其他定义与上述定义相似。最后，确定了平均总体准确性，以及无卒中个体、bs5 患者和 bs4 患者超过 30 次任务重复的准确性。

be
r
伯 of correct predictions by the number of observations
尔 正确的 根据观测次数作出的预测
3
ni j). Furthermore, the accuracy of
i=1 nii / i
j
classifica-
(1 = 1 nii/i j
此外，分类的准确性-

The classification was performed using the train function in R's *Caret* package. The training control is based on a fivefold crossvalidation scheme. For the KNN method, *tuneGrid* in the *Caret* package was applied such that the main parameters were decided automatically, and the value of *k* was set from 1 to 30. In accordance with a suggestion in [24], the radial basis function kernel was used for the SVM classification, and the

使用 r 的 Caret 包中的 train 函数进行分类。训练控制基于五重交叉验证方案。对于 KNN 方法，在 Caret 软件包中应用 tuneGrid，自动确定主要参数，并将 k 值设置为 1 一30。根据[24]中的建议，采用径向基函数核进行支持向量机分类，并采用径向基函数核进行支持向量机分类

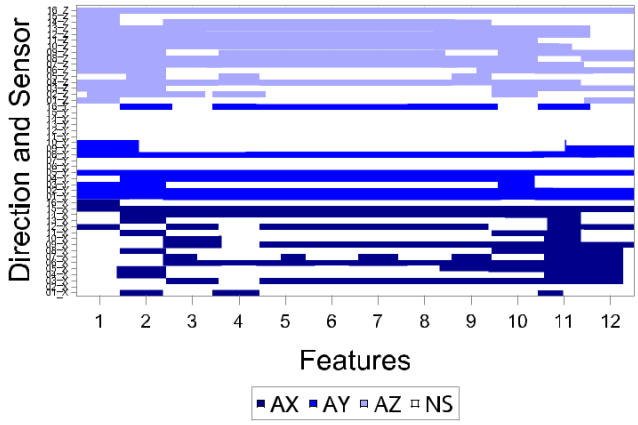

(a)

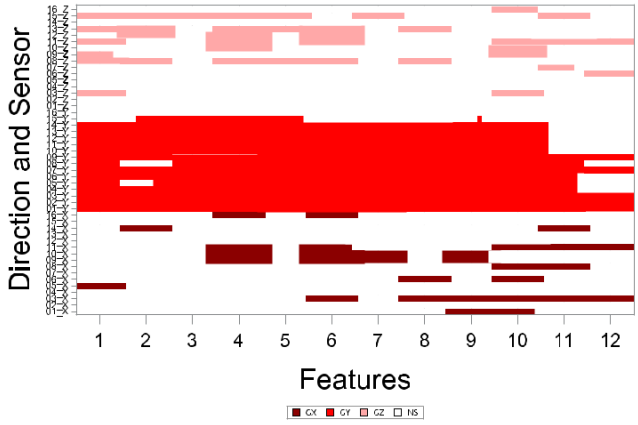

(b)

Fig. 7. Heat map of *p* values of features constructed from CI on the basis of GT data, where colored areas represent essential features from different sensors and directions for (a) A and (b) G. NS denotes nonsignificance.
图 7。根据 GT 数据从 CI 构建的特征的 p 值的热图，其中有色区域代表来自不同传感器和方向的基本特征(a) a 和(b) g。 NS 表示无意义。

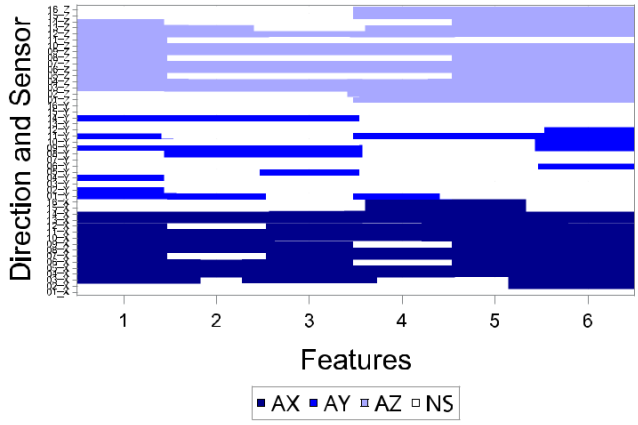

(a)

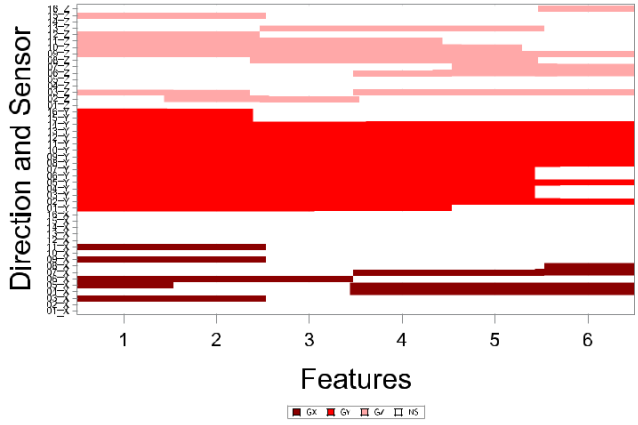

(b)

Fig. 8. Heat map of the *p* values of features constructed from CII on the basis of GT data, where colored areas represent essential features from different sensor and directions for (a) A and (b) G. NS denotes nonsignificance.
图 8。根据 GT 数据从 CII 构建的特征的 p 值的热图，其中有色区域代表来自(a) a 和(b) g。 NS 的不同传感器和方向的基本特征。

total number of unique combinations was set to 10 for the grid search. The cp value in *tuneGrid* under the DT method was set to apply searches from 0 to 0.005 in steps of 0.0005. The mtry value was set to 1:15 for *tuneGrid* under the RF method. Under the NB method, the rf parameter was set to search from 0 to 5 in steps of 1, the usekernel parameteer was set as TRUE, and the adjusted parameter was set to search from 0 to 5 in steps of 1. All these classification processes were repeated

网格搜索的独特组合总数被设置为 10。在 DT 方法下 tuneGrid 中的 cp 值被设置为以 0.0005 的步骤应用从 0 到 0.005 的搜索。在 RF 方法下，tuneGrid 的 mtry 值设置为 1:15。在 NB 方法下，将 rf 参数设置为从 0 到 5 的 1 步搜索，usekernel 参数设置为 TRUE，调整后的参数设置为从 0 到 5 的 1 步搜索。所有这些分类过程都是重复的

30 times to determine the final accuracy (*A*). Furthermore, the sample standard deviation (SD) of the accuracy level after 30 repetitions was obtained to derive the error interval for average accuracy, where the lower and upper bounds were was set to 0 when the computed lower bound was negative. When the computed upper bound exceeded 1, the upper bound was set to 1.

30 次，以确定最终的准确度(a)。此外，还得到了重复 30 次后精度水平的样本标准差(SD)，推导出了平均精度的误差区间，当计算的下界为负时，上下界设为 0。当计算的上限超过 1 时，上限设置为 1。

SD and A
A 1 96 SD 和 a 1 96 SD, respectively. The lower bound
标准差

III. Results
结果

A. Data Classification Involving Three Groups
涉及三组的数据分类

The essential features obtained from three constructions were used as classification inputs. Analyses were performed for each task as follows:

从三种结构中获得的基本特征作为分类输入，对每个任务进行如下分析:

1) TT: The average overall accuracy from 30 repetitions of the TT was computed, as indicated in Fig. 9 (a). The highest overall classification accuracy was that for CI, as determined by the KNN method, followed by that for CI and CII, as deter-mined by the SVM method. Regardless of the classification method used, the essential features in CI had the best classi-fication performance of all features. The classification ability from the use of essential CII and CIII features varied based on classification method. Under the KNN, DT, and NB methods, CI yielded a slightly higher accuracy than did CII and CIII. The error interval for CI under the KNN method was slightly shorter than those for the other methods, whereas the error intervals under the DT and NB methods were slight longer than those for the other methods. The error intervals derived from CI, CII, and CIII for the SVM and RF methods mostly overlapped. Under the KNN method, the error interval derived from CI was significantly higher that derived from CIII. Three error intervals for the DT method were siginificantly lower.

TT: 如图 9(a)所示，计算 30 次重复 TT 的平均总体准确性。总体分类精度最高的是用 KNN 方法确定的 CI，其次是用 SVM 方法确定的 CI 和 CII。无论使用何种分类方法，CI 中的基本特征在所有特征中具有最好的分类性能。使用基本 CII 和 ciiii 特征的分类能力根据分类方法而变化。在 KNN，DT 和 NB 方法下，CI 的准确性略高于 CII 和 CIII。与其他方法相比，KNN 方法的 CI 误差区间略短，DT 和 NB 方法的 CI 误差区间略长。来自 CI，CII 和 ciiii 的 SVM 和 RF 方法的误差区间大部分重叠。在 KNN 方法下，来自 CI 的误差区间显着高于来自 CIII 的误差区间。DT 方法的三个误差间隔显着较低。

Fig. 9 (b)–(d) presents the average accuracy in identifying individuals without stroke, patients with BS5, and patients with BS4. The highest average accuracy for individuals without

图 9(b)-(d)显示了识别无卒中个体、 bs5 患者和 bs4 患者的平均准确性。没有

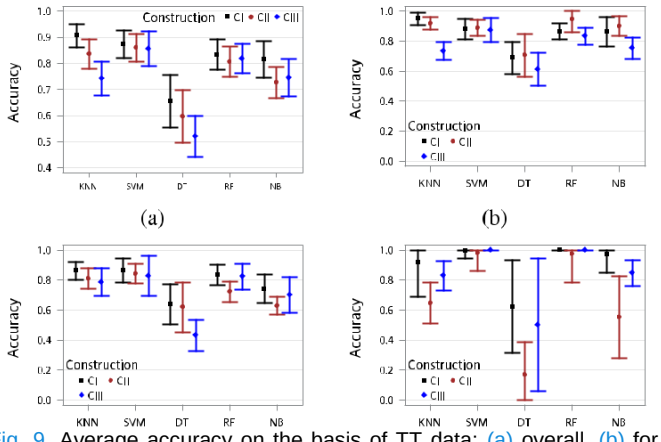

Fig. 9. Average accuracy on the basis of TT data: (a) overall, (b) for individuals without stroke, (c) for patients with BS5, and (d) for patients with BS4.

图 9。基于 TT 数据的平均准确性: (a)总体，(b)无卒中个体，(c) bs5 患者，(d) bs4 患者。

stroke was achieved using the RF method and essential CII features. The second highest accuracy was achieved using the KNN method and essential CI features. The performance of classification methods varied based on the construction of essential features. Except for when the the KNN and SVM methods were applied, the highest classification accuracy was observed when essential CII features were used. The essential CIII features had the poorest classification ability among all features. The error intervals for CI, CII, and CIII overlapped when the SVM method was applied, and the error interval was slightly shorter for CII than it was for CI and CIII. In particular, the lower bound of the error interval was very close to 0.8. The error interval derived from CII was slightly higher than those derived from CI and CIII when the RF method was used. The error interval of the average accuracy derived from CI and CII under the KNN method was significantly longer than that derived from CIII. The error interval was longer when the DT and NB methods were applied. The DT method provided significantly lower error intervals than did the other methods.

使用 RF 方法和基本的 CII 特征实现中风。使用 KNN 方法和基本 CI 特征实现了第二高的准确性。分类方法的性能根据基本特征的构建而变化。除了应用 KNN 和 SVM 方法时，使用基本 CII 特征时观察到最高的分类准确性。基本的 CIII 特征在所有特征中分类能力最差。应用支持向量机方法时，CI、 CII 和 CIII 的误差间隔重叠，CII 的误差间隔略短于 CI 和 CIII。特别是，误差区间的下限非常接近 0.8。当使用 RF 方法时，来自 CII 的误差间隔略高于来自 CI 和 CIII 的误差间隔。KNN 方法下 CI 和 CII 的平均准确度的误差间隔显着长于 CIII 的误差间隔。当应用 DT 和 NB 方法时，误差间隔更长。DT 方法提供的误差间隔显着低于其他方法。

The highest average accuracy with which the patients with BS5 were identified slightly exceeded 0.85, as indicated in Fig. 9 (c). Except for the DT and NB methods, the classifi-cation methods through which the essential CI features were input performed favorably. Classification method performance varied when the essential CII and CIII features were input. Under the RF and NB methods, the average accuracy for CIII was slightly higher than that for CII. Compared with individuals without stroke, the error interval was slightly longer for patients with BS5. Under the SVM and KNN methods, the error intervals for CI, CII, and CIII overlapped, but the error intervals for CII obtained from the SVM and KNN methods were shorter than those for CI and CII. The error intervals for CI and CIII under the RF method were slightly longer than the relevant error interval for CII. Under the DT and NB methods, the error intervals for CI, CII, and CIII overlapped.

如图 9(c)所示，bs5 患者的最高平均准确率略高于 0.85。除了 DT 和 NB 方法之外，输入基本 CI 特征的分类方法表现良好。当输入基本的 CII 和 ciiii 特征时，分类方法的性能变化。在 RF 和 NB 方法下，CIII 的平均准确性略高于 CII。与没有卒中的个体相比，bs5 患者的误差间隔略长。在支持向量机和 KNN 方法下，CI、 CII 和 CIII 的误差间隔是重叠的，但是由 SVM 和 KNN 方法得到的 CII 的误差间隔比 CI 和 CII 的误差间隔要短。RF 方法下 CI 和 CIII 的误差间隔略长于 CII 的相关误差间隔。在 DT 和 NB 方法下，CI，CII 和 CIII 的误差间隔重叠。

Only eight recordings were included for patients with BS4. Regardless of which construction was used, excellent

Bs4 患者仅包括 8 次记录。无论使用哪种结构，都很好

classification ability was noted for this group under the SVM and RF methods. Except for when the DT method was applied, the average accuracy for CI was >0.91. For CIII, the average accuracy was >0.81. When the essential CII features were input, classification was only successfully performed under the SVM and RF methods. Overall, the DT method had the poorest classification ability. The longest error interval was observed for patients with BS4. The upper bound for the KNN, SVM, and RF methods was set to 1, and the lower bound for the DT method was set to 0. The length of the error interval derived from CI and CIII under the RF method was close to

在支持向量机(SVM)和射频(RF)两种方法下，该组患者的分类能力明显增强。除了应用 DT 方法时，CI 的平均准确度 > 0.91。对于 ciiii，平均准确度 > 0.81。当输入基本的 CII 特征时，只有在 SVM 和 RF 方法下才能成功地进行分类。总体而言，DT 方法具有最差的分类能力。观察到 bs4 患者的最长误差间隔。KNN，SVM 和 RF 方法的上限设置为 1，DT 方法的下限设置为 0。在 RF 方法下从 CI 和 CIII 导出的误差区间的长度接近

0. That is, overfitting fitting was noted under the RF method for patients with BS4. Under the SVM method, the length of the error interval for CIII was close to 0, and the error intervals for CI and CII were slightly wider than that for CII. The KNN, DT, and NB methods provided a similar pattern of error intervals for CI, CII, and CIII, where the interval lengths derived from CIII for the KNN and NB methods and from CII for the DT method were slightly shorter. The performance of the DT method varied substantially across 30 repetitions.

也就是说，在 bs4 患者的 RF 方法下注意到过拟合。在支持向量机方法下，CIII 的误差区间长度接近于 0，CI 和 CII 的误差区间略宽于 CII。KNN、 DT 和 NB 方法为 CI、CII 和 CIII 提供了类似的误差间隔模式，其中从 CIII 得出的误差间隔长度对 KNN 和 NB 方法和从 CII 得出的误差间隔长度对 DT 方法略短。DT 方法的性能在 30 次重复中差异很大。

2) GT: Fig. 10 (a)–(d) presents the average accuracy of

GT: 图 10(a)-(d)表示

30 repetitions of the GT. The essential CI features under the SVM method had the highest overall average accuracy, followed by the essential CII features under the KNN method. Among constructions, the SVM method had the best classification ability. Except for those under the DT method, essential CI features had an average classification accuracy of >0.78. When the essential CII features were input, the average accuracy under the KNN and SVM methods was >0.84. Except for when the SVM method was used, the essential CIII features did not provide sufficient information to enable classification. The error interval patterns under the SVM, DT, and RF methods were similar. The error interval for CI was significantly higher than that for CIII. When the KNN method was used, the accuracy derived from three essential constructions differed significantly. The error interval derived from CII was higher than that from CI, and that from CIII was significantly lower. Most of the error intervals derived from CI, CII, and CIII overlapped under the NB method and the DT method.

GT 的重复。SVM 方法下的基本 CI 特征具有最高的总体平均精度，其次是 KNN 方法下的基本 CII 特征。在结构中，SVM 方法具有最好的分类能力。除了 DT 方法之外，基本 CI 特征的平均分类准确度 > 0.78。当输入基本的 CII 特征时，KNN 和 SVM 方法的平均准确度 > 0.84。除了使用支持向量机方法时，基本的 CIII 特征没有提供足够的信息来实现分类。SVM，DT 和 RF 方法下的误差区间模式是相似的。CI 的误差间隔显着高于 CIII。当使用 KNN 方法时，来自三个基本结构的准确性显着不同。来自 CII 的误差间隔高于来自 CI 的误差间隔，来自 CIII 的误差间隔显着降低。来自 CI，CII 和 CIII 的大部分误差区间在 NB 方法和 DT 方法下重叠。

Fig. 10 (b) presents the average accuracy for classifying individuals without stroke. When the essential CI features were used as inputs under the SVM method, the average accuracy was closer to 1. Except under the DT method, the average classification accuracy was >0.85 when the essential CI features were input, whereas that when the essential CII features were input was >0.80. The essential CIII features had the poorest classification ability of all features. The error intervals derived from CI under the SVM and RF methods were slightly longer than those from CII and CIII. The lower bound of the error interval for the SVM method exceeded

图 10(b)表示对没有中风的个体进行分类的平均准确性。当基本 CI 特征被用作 SVM 方法下的输入时，平均准确度接近 1。除 DT 法外，输入基本 CI 特征的平均分类精度 > 0.85，而输入基本 CII 特征的平均分类精度 > 0.80。基本的 CIII 特征在所有特征中分类能力最差。在支持向量机和 RF 方法下从 CI 得出的误差间隔略长于 CII 和 CIII。支持向量机方法的误差间隔下限超过

0.8. Under the KNN method, the lower bound of the error interval derived from CI and CII exceeded 0.8, whereas the upper bound under the error interval derived from CIII was close to 0.8. The patterns of error intervals under the DT and NB methods were similar.

8.在 KNN 方法下，由 CI 和 CII 导出的误差区间的下限大于 0.8，而由 CIII 导出的误差区间的上限接近于 0.8。DT 和 NB 方法下的误差间隔模式是相似的。

The average accuracy for classifying patients with BS5 was similar to that for classifying individuals without stroke. Under

Bs5 患者分类的平均准确性与无脑卒中患者分类的准确性相似

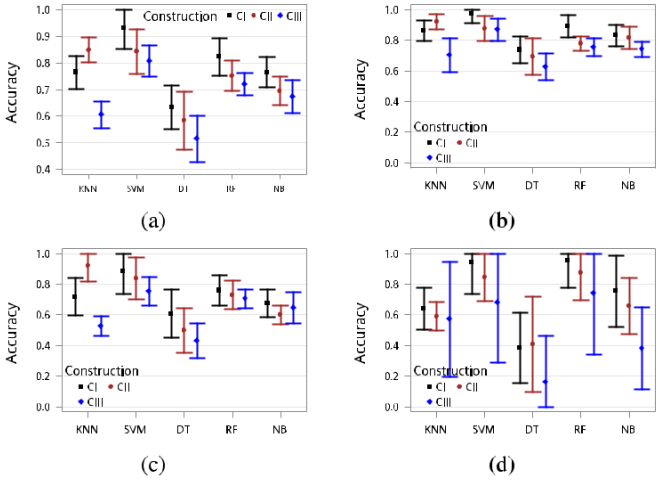

Fig. 10. Accuracy on the basis of the GT data: (a) overall, (b) for the individuals without stroke, (c) for the patients with BS5, and (d) for patients with BS4.
图 10。基于 GT 数据的准确性: (a)总体，(b)无卒中个体，(c) bs5 患者，(d) bs4 患者。

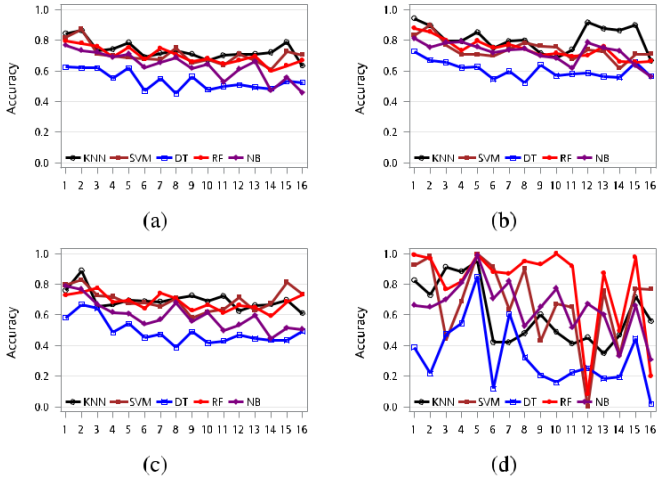

Fig. 11. Average accuracy of each sensor on TT in CI (a) all individuals, (b) individuals without stroke, (c) patients with BS5, and (d) patients with BS4.
图 11。 CI 中 TT 上每个传感器的平均准确度(a)所有个体，无脑卒中的个体，(c) bs5 患者，和(d) bs4 患者。

the SVM method, when essential CI features were used, the highest average accuracy of 0.88 was obtained, as indicated in Fig. 10 (c). When the essential CII features were used, the second highest average accuracy of 0.85 was obtained under the SVM method, and the third highest average accuracy was obtained under the KNN method. Regardless of construction, the RF and NB methods had average accuracy levels slightly exceeding 0.7 and 0.6, respectively. Three error intervals overlapped under the SVM, DT, RF, and NB methods, where the error interval derived from CI was slightly higher than those derived from CII and CIII. The error interval patterns derived CI, CIII and CIII under the KNN method were similar to those for the individuals without stroke.
支持向量机方法，当使用必要的 CI 特征时，最高平均准确度为 0.88，如图 10(c)所示。当使用基本 CII 特征时，SVM 方法的平均精度为 0.85，KNN 方法的平均精度为 0.85。无论结构如何，RF 和 NB 方法的平均精度水平分别略高于 0.7 和 0.6。三个误差区间在 SVM、 DT、 RF 和 NB 方法下重叠，其中 CI 的误差区间略高于 CII 和 CIII 的误差区间。KNN 方法得出的 CI，CIII 和 ciiii 的误差区间模式与没有卒中的个体相似。

Under the RF and SVM methods, when the essential CI features were used, the average accuracies obtained were approximately 1 and 0.94, respectively [Fig. 10 (d)]. Regardless of essential feature construction, the average accuracy under the RF method was >0.9. Classification was not possible under the DT method. The patterns of error intervals under the SVM and RF methods were similar. The interval derived from CI was significantly shorter that that derived from CIII. Under the KNN method, the the error intervals derived from CI and CII were significantly shorter than the interval derived from CIII. All the error intervals under the DT and NB methods were wide.

在 RF 和 SVM 方法下，当使用基本 CI 特征时，得到的平均准确度分别约为 1 和 0.94[图 10(d)]。对于基本特征构造较少的情况，RF 方法的平均准确度 > 0.9。在 DT 方法下分类是不可能的。SVM 和 RF 方法下的误差间隔模式是相似的。来自 CI 的间隔显着短于来自 CIII 的间隔。在 KNN 方法下，来自 CI 和 CII 的误差间隔显着短于来自 CIII 的间隔。DT 和 NB 方法下的所有误差间隔都很宽。

B. Sensor-Specific Classification Among Three Groups
B. 三组之间的传感器特定分类

The essential information derived from the sensor data varied with task design. The classification performance based on sensor data is discussed as follows. All of the features derived from CI were input.
从传感器数据中得到的基本信息随任务设计的不同而不同。基于传感器数据的分类性能讨论如下。来自 CI 的所有特征都被输入。

1) TT: Fig. 11 (a)–(b) presents the average classification accuracy for each sensor worn during the TT for the CI feature type.
TT: 图 11(a)-(b)显示了在 CI 特征类型的 TT 期间穿戴的每个传感器的平均分类准确性。

When the essential features derived from CI were used, the classification accuracy for most of the sensors was comparable under the KNN, SVM, and RF methods [Fig. 11 (a)]. The features derived from the data collected by sensors 1 and
当使用来自 CI 的基本特征时，大多数传感器的分类精度在 KNN、 SVM 和 RF 方法下是可比较的[图 11(a)]。来自传感器 1 和

2 provided valuable information for differentiation between participants. The average accuracy obtained under the KNN method was higher than those obtained under other methods for most sensor data. When sensors 6, 10, and 16 were excluded, the average accuracy was >0.7.

2 为参与者之间的区分提供了有价值的信息。KNN 方法获得的平均精度高于其他方法获得的大多数传感器数据的平均精度。当排除传感器 6,10 和 16 时，平均准确度 > 0.7。

Fig. 11 (b) presents the average accuracy obtained using the CI features for individuals without stroke. The highest average accuracy was again derived from the features extracted from data collected by sensors 1 and 2. The KNN method used features from sensor 1 data, and the SVM method used features from sensor 2 data. As for the features obtained from the data of most sensors, the KNN method had higher classification power than other methods. The performance of the SVM, RF, and NB methods was comparable for data collected by sensors other than sensors 1 and 2.

图 11(b)显示了没有中风的个体使用 CI 特征所获得的平均准确度。最高的平均准确度再次来源于从传感器 1 和 2 收集的数据中提取的特征。KNN 方法使用传感器 1 数据的特征，SVM 方法使用传感器 2 数据的特征。对于从大多数传感器的数据中获得的特征，KNN 方法比其他方法具有更高的分类能力。SVM，RF 和 NB 方法的性能与传感器 1 和 2 以外的传感器收集的数据相当。

The results related to average accuracy in classifying patients with BS5 are detailed in Fig. 11 (c). Data from sen-sor 2 provided more information than those from other sensors for identifying individuals in this group under the KNN and SVM methods. In contrast to the results for individuals without stroke, under the SVM method, features were derived from sensor 15 data. For the remaining sensor data, the performance of the KNN, SVM, and RF methods was comparable.

图 11(c)详述了与 bs5 患者分类的平均准确性有关的结果。来自传感器 2 的数据提供了比其他传感器更多的信息，用于根据 KNN 和 SVM 方法识别该组中的个体。与没有中风的个体的结果相反，在 SVM 方法下，特征来自传感器 15 数据。对于其余的传感器数据，KNN，SVM 和 RF 方法的性能是可比较的。

The performance of the methods varied considerably in classifying patients with BS4. For sensors 1, 2, 5, 8, 10, and 15, the RF method outperformed the other methods, and the average accuracy exceeded 0.95. For sensors 1, 2, 5, 6, and 8, the SVM method also yielded an average accuracy of >0.9. However, when sensor 12 data were used, differentiation between participants was not possible under the SVM and RF methods. When data from sensors 1, 3, 4, and 5 were used, the average accuracy obtained under the KNN method was >0.85. Finally, the NB method yielded a slightly higher average accuracy when data from sensors 4, 5, and 7 were used.

在对 bs4 患者进行分类时，这些方法的表现差异很大。对于传感器 1、2、5、8、10 和 15，RF 方法优于其他方法，平均精度超过 0.95。对于传感器 1,2,5,6 和 8，SVM 方法也产生了 > 0.9 的平均准确度。然而，当使用传感器 12 数据时，在 SVM 和 RF 方法下不可能区分参与者。当使用来自传感器 1,3,4 和 5 的数据时，在 KNN 方法下获得的平均准确度 > 0.85。最后，当使用来自传感器 4,5 和 7 的数据时，NB 方法产生略高的平均精度。

The average accuracy for each group for CII and CIII had similar patterns but was lower than the overall average accuracy (data not shown).

CII 和 ciiii 每组的平均准确性具有相似的模式，但低于总体平均准确性(数据未显示)。

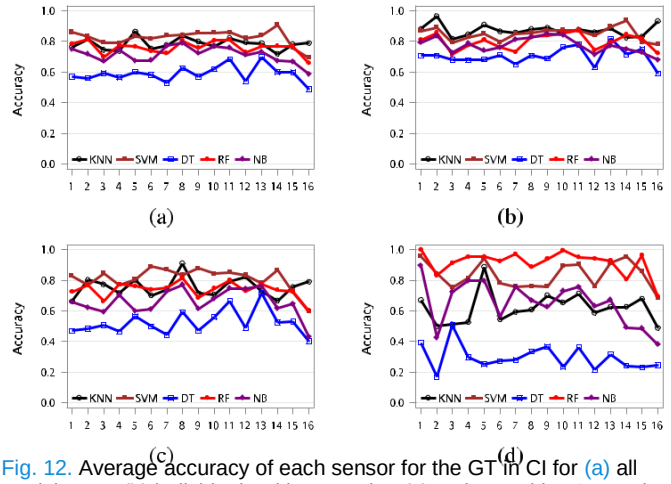

Fig. 12. Average accuracy of each sensor for the GT in CI for (a) all participants, (b) individuals without stroke, (c) patients with BS5, and (d) patients with BS4.
图 12。对于(a)所有参与者，(b)没有中风的个体，(c) bs5 患者，以及 Bs4 病人。

2) GT: Fig. 12 (a) presents the average accuracy for CI on the GT. Most of the sensor data provided sufficient information for the SVM method to differentiate between the participants. Almost all the sensor data had an average accuracy of >0.8. The performance of the KNN and RF methods was compara-ble, and the average accuracy slightly exceeded 0.75.

GT: 图 12(a)显示了 GT 上 CI 的平均准确性。大多数传感器数据为 SVM 方法提供了足够的信息来区分参与者。几乎所有的传感器数据的平均精度 > 0.8。KNN 和 RF 方法的性能是可比较的，平均精度略微超过 0.75。

The results related to the average accuracy in classi-fying individuals without stroke, patients with BS5, and patients with BS4 (using the CI features) are presented in Fig. 12 (b), (c), and (d), respectively.

图 12(b)、(c)和(d)分别给出了无脑卒中患者、 bs5 患者和 bs4 患者(使用 CI 特征)分类的平均准确性的结果。

The KNN and SVM methods identified individuals without stroke with high accuracy, as indicated in Fig 12 (b). The average classification accuracy under the KNN method was slightly higher, and features derived from sensor 2 data had the highest average classification accuracy. The highest average accuracy under the SVM method was achieved using features derived from sensor 14 data. The average accuracy under the RF method was 5% lower than that under the SVM method.

如图 12(b)所示，KNN 和 SVM 方法以高准确度鉴定没有卒中的个体。KNN 方法下的平均分类精度略高，来自传感器 2 数据的特征具有最高的平均分类精度。SVM 方法下的最高平均精度是使用来自传感器 14 数据的特征实现的。RF 方法的平均精度比 SVM 方法低 5% 。

Patients with BS5 were identified under the SVM method at an average accuracy of >0.85 [Fig. 12 (c)]. The features derived from data from sensors 9 and 14 provided sufficient information for classification. When the features derived from sensors 2, 5, 8, 11, and 12 were used, the KNN method had an average accuracy slightly exceeding 0.8. The average accuracy under the RF method slightly exceeded 0.7. The average accuracy under the DT method ranged from 0.4 to 0.6.

Bs5 患者在 SVM 方法下被识别，平均准确率 > 0.85[图 12(c)]。来自传感器 9 和 14 的数据的特征为分类提供了足够的信息。当使用来自传感器 2、5、8、11 和 12 的特征时，KNN 方法的平均精度略高于 0.8。RF 方法的平均精度略高于 0.7。DT 方法的平均精度在 0.4 到 0.6 之间。

The classification of patients with BS4 differed from that of the individuals without stroke, as indicated in Fig. 12 (d). When most of the sensor data were used, the highest average accuracy was achieved under the RF method; the average accuracy achieved was 1 when data from sensors 1 and 10 were used. The second highest average accuracy was obtained under the SVM method; the average accuracy was > 0.9 when features derived from sensors 1, 5, 11, and 13–15 were used. When features derived from sensor 1 data were used, the NB method had an average accuracy of 0.9. Under the DT method, the average accuracy was <0.5.

如图 12(d)所示，bs4 患者的分类与无卒中患者的分类不同。当使用大部分传感器数据时，射频方法的平均精度最高；当使用传感器 1 和 10 的数据时，平均精度为 1。支持向量机方法的平均精度仅次于传感器 1、5、11 和 13-15，平均精度 > 0.9。当使用来自传感器 1 数据的特征时，NB 方法的平均精度为 0.9。在 DT 方法下，平均准确度 < 0.5。

IV. Discussion
四、讨论

The approach of smoothing bases through regres-sion (smoothing) splines and Fourier bases (series) was used to extract features from accelerometer and gyroscope data. The hand function of patients with stroke was evaluated using the

通过回归(平滑)样条和傅里叶基(序列)来平滑基的方法被用来从加速度计和陀螺仪数据中提取特征。中风患者的手功能使用

TT and GT. According to the results, to differentiate between individuals without stroke, patients with BS4, and patients with BS5, CI coefficient estimates can be applied to either the TT or GT. For the TT, the coefficient estimates related to smoothing splines derived from sensors 1 and 2 were fairly accurate; for the GT, the corresponding estimates derived from sensor 14 data had the highest accuracy, followed by those derived from data from sensors 1, 5, and 9–11.

还有 GT。根据研究结果，为了区分无脑卒中患者、 bs4 患者和 bs5 患者，CI 系数估计可以应用于 TT 或 GT。对 TT 来说，从传感器 1 和 2 得到的与平滑样条相关的系数估计是相当准确的; 对 GT 来说，从传感器 14 得到的相应估计是最准确的，其次是从传感器 1、5 和 9-11 得到的数据。

Model performance was estimated using a fivefold cross-validation scheme and customized tuning grids. Furthermore, all processes were repeated 30 times to ensure the reliabil-ity of the classification result. For the TT, the KNN and SVM methods provided good classification accuracy when the essential features from CI were input. The KNN method had a slighter higher accuracy in identifying individuals without stroke, whereas the SVM method had higher accuracy in identifying patients With BS4. For the GT, the SVM method outperformed the other methods in terms of classification when essential CI features were used. In addition, although only eight recordings of patients with BS4 were included in this study, classification accuracy remained satisfactory under the SVM and RF methods. However, the DT method was not appropriate for use with imbalanced data.

使用五倍交叉验证方案和定制的调优网格估计模型性能。此外，所有过程重复 30 次，以确保分类结果的可靠性。对于 TT，当输入 CI 的基本特征时，KNN 和 SVM 方法提供了良好的分类准确性。KNN 方法在识别无卒中的个体方面具有较高的准确性，而 SVM 方法在识别 bs4 患者方面具有较高的准确性。对于 GT，当使用基本 CI 特征时，SVM 方法在分类方面优于其他方法。此外，虽然本研究仅包括 8 例 bs4 患者的记录，但在 SVM 和 RF 方法下分类准确性仍然令人满意。然而，DT 方法不适合用于不平衡的数据。

Although participants were asked to perform the task repeatedly, some time gaps remained between repetitions. The cyclical characteristics of sample data remained somewhat unclear. Consequently, the lowest classification accuracy was achieved when CIII features were used. Thus, for similar experiments, the extraction of features for each cycle is advised. Furthermore, the CI and CII features were derived by computing the average coefficient estimates for ten cycles. Since the data trajectories of patients with BS4 or BS5 was not as regular as that of individuals without stroke, the variability levels in coefficient estimates for ten cycles can be treated as potential features for classification in addition to averages for summarizing features.

虽然参与者被要求重复执行这项任务，但是在重复之间仍然存在一些时间间隔。样本数据的周期性特征仍然有些不清楚。因此，当使用 CIII 特征时，分类准确性最低。因此，对于类似的实验，建议提取每个周期的特征。此外，CI 和 CII 特征是通过计算十个周期的平均系数估计值得出的。由于 bs4 或 bs5 患者的数据轨迹不如无卒中个体的规则，因此除了总结特征的平均值外，10 个周期系数估计值的变异水平可以作为潜在的分类特征。

The number of degrees of freedom selected for functional form was restricted because the number of variables already considerably exceeded the number of participants. If a larger sample size is employed, the model accuracy can be improved using a more complex functional form. The functional form of our accelerometer and gyroscope data was nonperiodic. Because a Fourier series was designed to model the cyclical data, a wavelet series may also be applicable for these data.

为功能形式选择的自由度数量受到限制，因为变量的数量已经大大超过了参与者的数量。如果采用更大的样本量，则可以使用更复杂的函数形式来提高模型的准确性。我们的加速度计和陀螺仪数据的函数形式是非周期性的。因为傅里叶级数是用来模拟周期性数据的，所以小波级数也可能适用于这些数据。

Table III details the methods used in [16], [18], [25], [26] and the current method for comparison. In [16], the researchers directly extracted features from the movement characteristics of each participant. By contrast, [18] computed summary statistics in terms of centrality and variability in each cycle to extract raw data from each task. To reduce the number of features, an independent-samples *t*-test and PCA were performed, and the features derived from the PCA were

表三详细说明了[16]、[18]、[25]和[26]中使用的方法以及目前的比较方法。在[16]中，研究人员直接从每个参与者的运动特征中提取特征。相比之下，[18]根据每个周期的中心性和可变性计算总结统计，以从每个任务中提取原始数据。为了减少特征的数量，进行独立样本 t 检验和 PCA，并且来自 PCA 的特征是

TABLE III
表三
DETAILS OF PREVIOUS METHODS AND THE PROPOSED
以往方法的详情及建议的
METHOD FOR COMPARISON
比较方法

	[16]	[18]	[25]	[26]	Proposed method
Tasks	TT, GT and CTT	TT, GT and CTT	Random movement motor task	Finger-to-nose task	TT and GT
Feature extraction	Processing of kinematic parameters	Kinematic parameters	Kinematic parameters	Kinematic parameters	Functional form
Feature selection	None	PCA	Statistical extraction	Statistical extraction	One-way ANOVA and Wilcoxon test
Important features					
Important sensor position	No	Indirect	No	No	Direct
Important task	No	Yes	No	No	Yes
Mapped clinical scale	Brunnstrom stage	Brunnstrom stage	Fugl-Meyer assessment scores	FMA-UE, ARAT and MBI	Brunnstrom stage
Results	Accuracy = 70.22%	No	$r^2 = 0.70$	55%, 51% and 32% of variance in FMA-UE, ARAT and MBI, respectively	Accuracy $> 90\%$

linear combinations of summary statistics of centrality and variability. Notably, the summary statistics, especially those for variability, were highly sensitive to outliers. [25] and [26] have extracted motion periodic motion parameters as features and then used statistical methods, such as the Kruskal–Wallis test, for feature selection. Under these methods, features with repeated effects may be selected, which in turn affects the prediction effect of the classifier. However, in the proposed method, a functional form was fitted to the trajectory of each cycle in each task. The features, which are coefficient estimates, represent the direct characteristics of functional forms. Furthermore, generalized crossvalidation was conducted to determine the number of parameters that in turn determined the smoothness of data trajectories. Unlike the summary statistics computed from all sample data, the proposed method used the coefficients of the smoothed curve and hence the outliers had a negligible influence on the features.

汇总统计的中心性和可变性的线性组合。值得注意的是，总结统计，特别是变异性统计，对异常值高度敏感。[25]和[26]提取运动周期运动参数作为特征，然后使用统计学方法，如 Kruskal-Wallis 检验，进行特征选择。在这些方法下，可以选择具有重复效应的特征，这反过来影响分类器的预测效果。然而，在所提出的方法中，每个任务的每个周期的轨迹都拟合了一个函数形式。这些特征是系数估计，代表了函数形式的直接特征。此外，进行广义交叉验证以确定参数的数量，这些参数又决定了数据轨迹的平滑性。与从所有样本数据中计算出来的总结统计量不同，该方法使用了光滑曲线的系数，因此异常值对特征的影响可以忽略不计。

As discussed in [18] and as determined through variable loading in the PCA, the most critical sensor position was indirect, and only features obtained from the TT could distinguish between patients with BS5 and BS4. However, the proposed method of constructing features was effective at classifying patients' BS and identifying the important position

正如文献[18]中所讨论的那样，通过 PCA 中的可变负荷来确定，最关键的传感器位置是间接的，只有从 TT 中获得的特征才能区分 bs5 和 bs4 患者。然而，所提出的构建特征的方法在分类患者的 BS 和确定重要位置方面是有效的

TABLE IV
表四
ACCURACY UNDER VARIOUS CLASSIFICATION METHODS ON TT AND THE GT
TT 和 GT 在不同分类方法下的准确性

		Sensors									
TT	H BS5	2,1	3,0 1,1	0,1	1,1	1,0	1,0	1,0	1,0	1,0 0,1	

Note : x and y

0.85, respectively.

of sensors on the data glove. Table IV presents a summary, for each sensor in each task, of the number of classification methods under which the average group accuracy was higher than 0.85 and between 0.8 and 0.85 when CI features were used. For the TT, the information provided by sensor 2 was the most useful for classification, followed by the information provided by sensors 5, 1, 8, and 15. When the thumb was pressing a button, sensors 1 and 2 captured larger movements, sensor 15 captured muscle movements, and sensor 5 generated a signal upon impact or contact with the thumb. Determined according to physical principles, the order of inference effects is as follows: sensor 1 > sensor 2 > sensor 15 > sensor 5. Sensor 1 was positioned at the fingertips and was therefore easily affected by the sliding of a glove and by the reaction force generated from pressing a button. Moreover, the amount of noise was relatively large, meaning that the related effect may have been reduced. In the GT, differentiation between groups was possible under most of classification methods when features derived from sensors 1, 5, 8, 10, and 11 were used. Sensor 16 was designed as a reference for computing another measurement and was demonstrated to be unimportant. Per physical principles, inference effects were expected to be strongest under sensors 1, 3, 6, 9, and 12, which were positioned on the fingertips. However, a similar problem as that encountered with the TT occurred: the fingertip sensors were susceptible to sliding of gloves and the reaction force generated by gripping. Furthermore, the amount of noise was relatively large, meaning that the effect may have been reduced. Sensor 1 captured a larger range of motion during the GT, meaning that it was the most effective sensor overall, followed by sensors 5, 8, 11, and 14, which were positioned at the base of the fingers. The position in sensor 1 in the rankings was pushed back once more because the movement of the little finger was too small.

数据手套上的传感器。表四列出了每个任务中每个传感器的分类方法的总数，当使用 CI 特征时，分类方法的平均分组精度高于 0.85，在 0.8 至 0.85 之间。对于 TT，传感器 2 提供的信息对分类最有用，其次是传感器 5、1、8 和 15 提供的信息。当拇指按下按钮时，传感器 1 和 2 捕捉更大的运动，传感器 15 捕捉肌肉运动，传感器 5 在碰撞或与拇指接触时产生信号。根据物理原理确定，推断效果的顺序如下：传感器 1 > 传感器 2 > 传感器 15 > 传感器 5。传感器 1 位于指尖，因此容易受到手套滑动和按下按钮产生的反作用力的影响。此外，噪音的数量相对较大，这意味着相关的影响可能已经减少。在 GT 中，当使用来自传感器 1、5、8、10 和 11 的特征时，大多数分类方法都可以区分不同的组。Sensor 16 被设计为计算另一个测量的参考，并被证明是不重要的。根据物理原理，推理效果预计是最强的传感器 1,3,6,9 和 12，这是定位在指尖。然而，与 TT 遇到的类似问题发生了：指尖传感器易于滑动手套和握持产生的反作用力。此外，噪音量相对较大，这意味着效果可能已经降低。传感器 1 捕获了更大范围的运动在燃气轮机，这意味着它是最有效的传感器总体上，其次是传感器 5,8,11 和 14，这是定位在根部的手指。排名中传感器 1 的位置再次被推后，因为小手指的运动太小了。

Owing to the design of the data grove, the current study can only be used to evaluate patients with minor motor impairment, such as patients with BS4 to BS6. For patients with severe motor impairment, the priority of rehabilitation should be focused on movements of the entire upper limbs. Other device designs might be required. Furthermore, because of the inconsistent number of recordings in the TT and GT, the data for the TT and GT could not be merged. In future

由于数据树的设计，目前的研究只能用于评估轻微运动障碍患者，如 bs4 至 bs6 患者。对于严重运动功能障碍的患者，康复的重点应该放在整个上肢的运动上。可能需要其他设备设计。此外，由于 TT 和 GT 中记录的数量不一致，TT 和 GT 的数据无法合并。在未来

studies, the number of recordings for each task should be set to be consistent such that multitask integration can be performed.
研究中，每个任务的录音数量应设定为一致，以便能够进行多任务整合。

V. Conclusion
结论

In accordance with the results of this study, functional analysis can be used to model the trajectory of data colllected by IMU sensors, and the corresponding coefficients can be treated as features for evaluating hand function. The GT task provided more sophisticated features to distinguish the extent of the hand function determined by BS. When the GT was used, the features had average accuracies of over 0.9 under the SVM method. When only data from sensors 1, 5, 8, 10, and 11 were used, the average accuracy was also over 0.91. Thus, in future data glove systems, only six sensors can be used, and a functional analysis model can be used to extract the features for evaluating hand function and formulating rehabilitation plans.

根据本文的研究结果，功能分析可以用来模拟 IMU 传感器采集的数据的轨迹，并且相应的系数可以作为评价手功能的特征。GT 任务提供了更复杂的特征来区分 BS 确定的手功能的程度。当使用 GT 时，在支持向量机方法下，特征的平均准确度超过 0.9。当只使用传感器 1、5、8、10 和 11 的数据时，平均精度也超过 0.91。因此，在未来的数据手套系统中，只能使用六个传感器，并且可以使用一个功能分析模型来提取特征，用于评估手功能和制定康复计划。

References
参考文献

[1] World Health Organization. *WHO Reveals Leading Causes of Death and Disability Worldwide 2000–2019*. Accessed: Dec. 9, 2020. [Online]. Available: https://www.who.int/news/item/09-12-2020-who-reveals-leading-causes-of-death-and-disability-worldwide-2000-2019
世界卫生组织。WHO 揭示 2000-2019 年世界范围内主要死亡和残疾原因。获取：2020 年 12 月 9 日。[在线]。可获得：https://www.who.int/news/item/09-12-2020-who-reveals-leading-causes-of-death-and-disability-worldwide-2000-2019
[2] Ministry of Health and Welfare. *Taiwan's Leading Causes of Death in 2020*. Accessed: Jun. 18, 2020. [Online]. Available: https://www.mohw.gov.tw/cp-5017-61533-1.html
卫生福利部。2020 年台湾主要死亡原因。访问: 2020 年 6 月 18 日
[3] Y. John and F. Anne, "Review of stroke rehabilitation," *BMJ*, vol. 334, no. 7584, pp. 86–90, 2007.
《中风康复评论》，英国医学杂志，第 334 卷，第 7584 页，第 86-90 页，2007 年。
[4] Z. Yue, X. Zhang, and J. Wang, "Hand rehabilitation robotics on poststroke motor recovery," *Behav. Neurol.*, vol. 2017, Nov. 2017, Art. no. 3908135.
医疗照护机器人在中风后运动恢复中的作用。Neurol，2017 卷，2017 年 11 月，艺术。第 3908135 号。
[5] R. Stockley, R. Peel, K. Jarvis, and L. Connell, "Current therapy for the upper limb after stroke: A cross-sectional survey of U.K. Therapists," *BMJ Open*, vol. 9, no. 9, 2018, Art. no. e030262.
斯托克利，r。皮尔，k。贾维斯和 l。康奈尔，"中风后上肢的当前治疗：英国治疗师的横断面调查"，英国医学杂志开放版，2018 年第 9 卷，艺术。不。E030262.
[6] T. Platz, C. Pinkowski, F. van Wijck, I.-H. Kim, P. di Bella, and G. Johnson, "Reliability and validity of arm function assessment with standardized guidelines for the fugl-meyer test, action research arm test and box and block test: A multicentre study," *Clin. Rehabil.*, vol. 19, no. 4, pp. 404–411, Jun. 2005.
平可夫斯基，范维克，I.-H。符合 fugl-meyer 测试、动作研究手臂测试和方块测试标准化指南的手臂功能评估的可靠性和有效性：一项多中心研究。Rehabilitation，第 19 卷，第 4 号，第 404-411 页，2005 年 6 月。
[7] L. Yu, J. P. Wang, Q. Fang, and Y. Wang, "Brunnstrom stage automatic evaluation for stroke patients using extreme learning machine," in *Proc. IEEE Biomed. Circuits Syst. Conf. (BioCAS)*, Hsinchu, Taiwan, Nov. 2012, pp. 380–383.
余丽萍，王建平，王庆芳，王永，《使用极限学习机器对脑卒中患者进行 Brunnstrom 阶段自动评估》，见 Proc。IEEE 生物医学。电路系统。参考文献。新竹，台湾，2012 年 11 月，第 380-383 页。
[8] J. Stamatakis *et al.*, "Finger tapping clinimetric score prediction in Parkinson's disease using low-cost accelerometers," *Comput. Intell. Neurosci.*, vol. 2013, Art. no. 717853.
Stamatakis et al。，"使用低成本加速度计进行帕金森病的手指敲击临床评分预测。"。英特尔。神经科学，2013 年第一卷，艺术。第 717853 号。
[9] M. Djuri`c-Jovi`ci` *et al.*, "Finger tapping analysis in patients with Parkin-son's disease and atypical parkinsonism," *J. Clin. Neurosci.*, vol. 30, pp. 49–55, Aug. 2016.
Djuri' c-jovi ci' et al。，"帕金森病和非典型帕金森综合征患者的手指敲击分析"，j. lin。神经科学，第 30 卷，第 49-55 页，2016 年 8 月。

[10] Y. Sano *et al.*, “Quantifying Parkinson’s disease finger-tapping severity by extracting and synthesizing finger motion properties,” *Med. Biol. Eng. Comput.*, vol. 54, no. 6, pp. 953–965, Jun. 2016.

Y. Sano 等，“通过提取和合成手指运动特性来量化帕金森病手指敲击的严重程度”，Med。生物学。英文版。计算机，第 54 卷，第 6 期，第 953-965 页，2016 年 6 月。

[11] H. Dai, P. Zhang, and T. C. Lueth, “Quantitative assessment of parkinsonian tremor based on an inertial measurement unit,” *Sensors*, vol. 15, no. 10, pp. 25055–25071, 2015.

戴秉国，张平，和 T.C.Lueth，“基于惯性导航系统的帕金森氏震颤定量评估”，《传感器》，第 15 卷，第 10 期，第 25055-25071 页，2015 年。

[12] W. W. Lee *et al.*, “A smartphone-centric system for the range of motion assessment in stroke patients,” *IEEE J. Biomed. Health Informat.*, vol. 18, no. 6, pp. 1839–1847, Nov. 2014.

Lee 等人，“一个以智能手机为中心的中风患者运动评估范围系统,”IEEE j。 Biomed。健康信息，第 18 卷，第 6 期，第 1839-1847 页，2014 年 11 月。

[13] V. Venkataraman *et al.*, “Component-level tuning of kinematic features from composite therapist impressions of movement quality,” *IEEE J. Biomed. Health Informat.*, vol. 20, no. 1, pp. 143–152, Jan. 2016.

Venkataraman 等，“从复合治疗师对运动质量的印象中调整运动学特征的组件级别,”ieeej.Biomed。健康信息，第 20 卷，第 1 期，第 143-152 页，2016 年 1 月。

[14] P. Xia, T. Ding, Y. Peng, Q. Yang, and J. Li, “A multi-information data glove for hand function evaluation of stroke patients,” *Investigación Clínica*, vol. 61, no. 1, pp. 328–339, Mar. 2020.

夏碧霞，丁丁，彭，杨，李，“一个用于脑卒中患者手功能评估的多信息数据手套”，《临床研究》，第 61 卷，第 1 期，第 328-339 页，2020 年 3 月。

[15] H. G. Kortier, V. I. Sluiter, D. Roetenberg, and P. H. Veltink, “Assessment of hand kinematics using inertial and magnetic sensors,” *J. Neuroeng. Rehabil.*, vol. 11, no. 1, pp. 1–15, Dec. 2014.

鲁腾伯格和威尔廷克，“使用惯性和磁性传感器评估手的运动学”，j。《康复》，第 11 卷，第 1 期，第 1 至 15 页，2014 年 12 月。

[16] B.-S. Lin, P.-C. Hsiao, S.-Y. Yang, C.-S. Su, and I.-J. Lee, “Data glove system embedded with inertial measurement units for hand function evaluation in stroke patients,” *IEEE Trans. Neural Syst. Rehabil. Eng.*, vol. 25, no. 11, pp. 2204–2213, Nov. 2017.

B.-S.林炳泉。萧美儿。杨先生。Su 和 i-j。Lee，“嵌入惯性测量单元的数据手套系统用于中风患者的手功能评估,”IEEE Trans。神经系统。康复。2017 年 11 月，第 25 卷，第 11 页，2204-2213 页。

[17] B.-S. Lin, I.-J. Lee, P.-Y. Chiang, S.-Y. Huang, and C.-W. Peng, “A modular data glove system for finger and hand motion capture based on inertial sensors,” *J. Med. Biol. Eng.*, vol. 39, no. 4, pp. 532–540, Aug. 2019.

B.s.林，I.-J。李佩儿。蒋学礼。黄志光，以及 c. w。彭，“一个基于惯性传感器的手指和手部运动捕捉的模块化数据手套系统,”j。生物学。2019 年 8 月，第 39 卷，第 4 期，532-540 页。

[18] B.-S. Lin, I.-J. Lee, P.-C. Hsiao, and Y.-T. Hwang, “An assessment system for post-stroke manual dexterity using principal component analysis and logistic regression,” *IEEE Trans. Neural Syst. Rehabil. Eng.*, vol. 27, no. 8, pp. 1626–1634, Aug. 2019.

译注:。林，I.-J。李永平。萧永泰及 y.t。使用主成分分析和 logit 模型的脑卒中后手的灵活性评估系统。神经系统。康复。2019 年 8 月，第 27 卷，第 8 页，1626-1634 页。

[19] B. S. Lin, Y. S. Lin, I. J. Lee, and B. S. Lin, “A real-time missing data recovery method using recurrent neural network for multiple transmissions,” in *Recent Advances in Intelligent Information Hiding and Multimedia Signal Processing*, J. S. Pan, A. Ito, P. W. Tsai, and L. C. Jain, Eds. Cham, Switzerland: Springer, 2019, pp. 99–107.

Lin，y. s. Lin，I.j. Lee，and B.s. Lin，“一种使用递归神经网络进行多次传输的实时缺失数据恢复方法”，见于智能信息隐藏和多媒体信号处理的最新进展，J.s. Pan，a. Ito，p. w. Tsai 和 L.c. Jain，Eds。瑞士占: 斯普林格出版社，2019 年，第 99-107 页。

[20] A. Hua *et al.*, “Evaluation of machine learning models for classify-ing upper extremity exercises using inertial measurement unit-based kinematic data,” *IEEE J. Biomed. Health Informat.*, vol. 24, no. 9, pp. 2452–2460, Sep. 2020.

Hua 等，“使用基于惯性测量单元的运动学数据对上肢运动进行分类的机器学习模型的评估”，IEEE j. Biomed。健康信息，第 24 卷，第 9 期，第 2452-2460 页，2020 年 9 月。

[21] J. O. Ramsay and B. W. Silverman, *Applied Functional Data Analysis: Methods and Case Studies*. New York, NY, USA: Springer, 2002.

应用功能数据分析: 方法与案例研究。纽约，纽约，美国: Springer，2002。

[22] R. L. Eubank, *Nonparametric Regression Spline Smoothing*, 2nd ed. New York, NY, USA: Marcel Dekker, 1999.

Eubank，非参数回归样条平滑，第 2 版。纽约，纽约，美国: Marcel Dekker，1999。

[23] A. Tharwat, “Classification assessment methods,” *Appl. Comput. Inf.*, vol. 17, no. 1, pp. 168–192, 2021.

《分类评估方法》，计算机应用资料，第 17 卷，第 1 期，第 168-192 页，2021 年。

[24] G. L. Prajapati and A. Patle, “On performing classification using SVM with radial basis and polynomial kernel functions,” in *Proc. 3rd Int. Conf. Emerg. Trends Eng. Technol.*, Nov. 2010, pp. 512–515.

Prajapati 和 a。 Patle，“关于使用径向基和多项式核函数的支持向量机进行分类”，在 Proc 中。第三国际。参考文献。Emerg 紧急情况。Trends Eng 趋势。Technol。，2010 年 11 月，512-515 页。

[25] B. Oubre *et al.*, “Estimating upper-limb impairment level in stroke survivors using wearable inertial sensors and a minimally-burdensome motor task,” *IEEE Trans. Neural Syst. Rehabil. Eng.*, vol. 28, no. 3, pp. 601–611, Mar. 2020.

使用可穿戴的惯性传感器和最小负担的运动任务估计中风幸存者的上肢损伤程度。神经系统。康复。2020 年 3 月，第 28 卷，第 3 期，第 601-611 页。

[26] Z.-J. Chen, C. He, M.-H. Gu, J. Xu, and X.-L. Huang, “Kinematic evaluation via inertial measurement unit associated with upper extremity motor function in subacute stroke: A cross-sectional study,” *J. Healthcare Eng.*, vol. 2021, pp. 1–7, Aug. 2021.

Z-j.陈，c，何，m.h。顾先生、徐先生、徐先生、徐先生。通过惯性导航系统对亚急性脑卒中患者上肢运动功能的运动学评估: 横向研究。